CloudSat Project

A NASA Earth System Science Pathfinder Mission

Level 2 GEOPROF Product Process Description and Interface Control Document Algorithm version 5.3

Date: 28 June 2007

Address questions concerning the document to:

Gerald Mace
mace@met.utah.edu
(801) 585-9489

Contents

1. Introduction

The presence or absence and vertical location of cloud layers impose powerful constraints on the radiative properties of an atmospheric column and, thereby, modulate strongly the radiative heating rate of the column. Comprehensive information on the vertical distribution of cloud layers have been largely missing from analyses of conventional passive-sensor satellite radiometers that observe only the emitted and reflected radiance from the atmosphere and surface. Conventional satellite data have only allowed us to crudely estimate the location and vertical extent of clouds. Active remote sensors such as CloudSat, on the other hand, are uniquely adapted to observe the vertical location of hydrometeor layers. Therefore, a basic requirement of the CloudSat project is to use data from the Cloud Profiling Radar (CPR) to identify those levels in the vertical column sampled by CloudSat that contain significant radar echo from hydrometeors and to produce an estimate of the radar reflectivity factor for each volume deemed to contain significant echo (Stephens et al, 2001).

The CloudSat orbit will follow closely the orbit of the EOS PM1 satellite (Aqua) on which a number of advanced passive remote sensors will observe the earth. This synergistic association can add significantly to our understanding of the CloudSat geometrical profile and we will use this data source to our advantage. In particular, the Moderate-Resolution Imaging Spectroradiometer (MODIS) will provide information regarding the occurrence and horizontal distribution of clouds within the CloudSat footprint. The MODIS cloudmask product (Ackerman et al., 1998) will be available for use in the operational CloudSat processing stream. The MODIS cloudmask contains not only an estimate of the likelihood of clouds in 1km MODIS pixels, but also contains the results of a number tests with MODIS-observed spectral radiances that will provide limited information on the nature of the clouds in the vertical column. We will use the results of these tests to help us evaluate the characteristics of the CPR hydrometeor returns by performing comparisons of the CPR hydrometeor mask and the MODIS spectral tests.

This document describes the algorithm that will be implemented operationally to identify significant radar echo in the CloudSat data stream. The goals of the algorithm are to

- Examine the characteristics of each range resolution volume to determine if the radar data for that volume is significantly different from the radar noise characteristics and, thus, deemed to contain hydrometeors,
- Quantify the likelihood that a given range resolution volume with characteristics different from noise actually contains hydrometeors,
- Compare the radar significant echo profile with the information from the MODIS cloud mask.

2. *Algorithm Theoretical Basis*

The Geometrical Profile (GEOPRO) algorithm will contain two parts. The first part will be designed to identify significant radar echo in profiles of returned radar power in the CloudSat CPR data. The second part will consist of a comparison of the geometrical profile algorithm with the MODIS cloud mask spectral tests. This comparison will allow for an initial comparison of the CloudSat profile and the MODIS cloud mask.

2.1 The Significant Echo Mask Algorithm

The CPR records range-resolved profiles of backscattered power. These measurements as contained in the level 1B input data represent a 0.16 s average of returned power that correspond nominally to a horizontal resolution of 2.5 km along track by 1.2 km across track. The range resolution is 500 m and will be oversampled to generate a range gate spacing of 250m.

The goal of the significant echo mask (SEM) portion of the GeoProf algorithm is to identify those resolution volumes that contain signal that is significantly different from noise and establish the likelihood that such volumes contain hydrometeors. The goal of the SEM algorithm is to maximize the identification of hydrometeor echo while minimizing the occurrence of false alarms (false alarms are defined as range resolution volumes identified as contain hydrometeor return when none actually exits). Since the CPR minimum detectable signal is -28 dBZ_e, some hydrometeor layers will have a backscatter crosssection per unit volume that generates signal near or below the detection threshold of the CPR. It is necessary, therefore, to carefully tune the SEM to extract all possible significant signals from the radar returns. In formulating the SEM, we will generally follow the approach outlined by Clothiaux et al (1995 and 2000) with some modifications as described below. The level 1b data that will be available to the GEOGROF algorithm will include the power return $P_{r,jk}$ in each resolution volume where subscript j defines the along track dimension and k the vertical dimension. Given the pulse repetition frequency of 4300 Hz, and the averaging time of 0.16s, $P_{r,jk}$, represents an average of nominally 688 pulses. The measured value is composed of a sum of power return from the atmosphere ($P_{h,jk}$) and a Gaussian-like background system noise power ($P_{n,jk}$) assumed to be due primarily to the mixer noise. Our initial criteria for a significant return is that $P_{r,jk} > P_{n,jk}+(3\sigma_n)$ where σ_n is the standard deviation of $P_{n,jk}$ estimated by examining P_n in nearby regions above the tropopause where we are certain no atmospheric return will be recorded in the reported values $P_{r,jk}$. If the noise characterization is accurate and Gaussian, approximately 0.25% of noise returns will be incorrectly labeled as significant echo, P_{sig}. While we can be certain that while there will be few occurrences where noise will be identified as significant, there will be hydrometeor returns where $P_{h,jk} < P_{n,jk}+(3\sigma_n)$. One of the major goals of the GEOPROF algorithm is to accurately identify these volumes.

In an effort to identify the relatively weak but significant radar returns, we will implement a statistical approach that effectively increases the separation between signal

and noise by assuming some degree spatial and vertical continuity of the hydrometeor field on the scales of the CloudSat observations. Consider a two-dimensional data window m resolution volumes along track and n resolution volumes in depth centered on some pixel whose power value is $P_{r,jk} < P_{n,jk} + (3\sigma_n)$. We can ascertain the likelihood of this resolution volume not containing significant radar echo by comparing the statistics of that pixel and its neighbors to the estimate of the noise statistics acquired from pixels known to not contain significant echo. The Gaussian probability that the pixel is noise
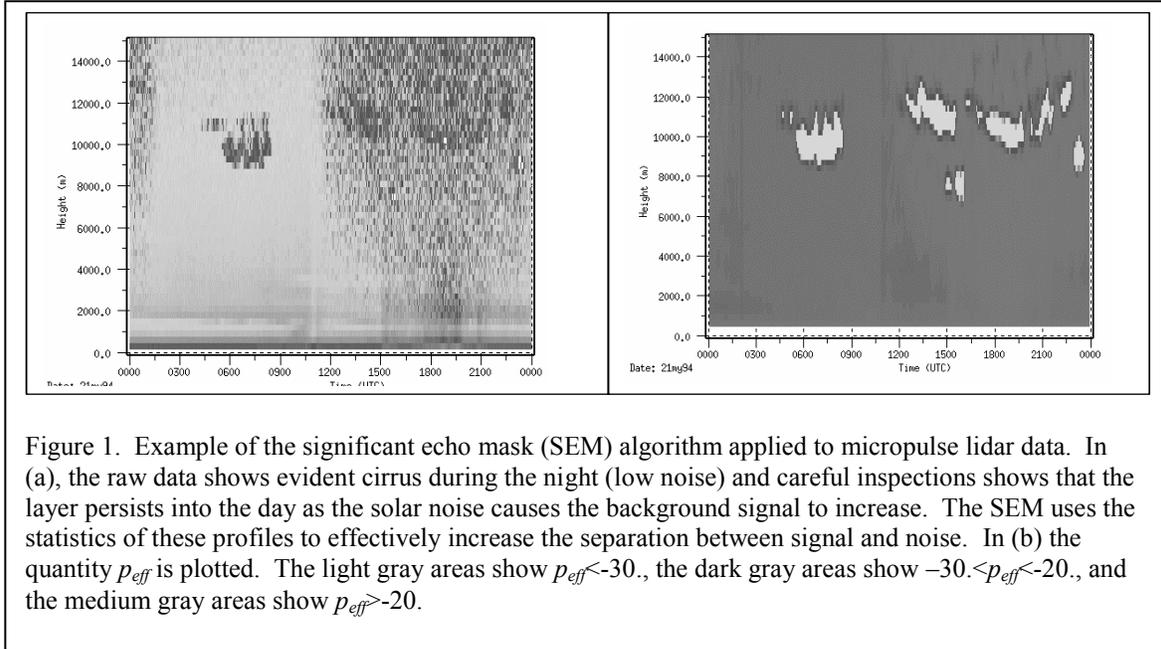

Figure 1. Example of the significant echo mask (SEM) algorithm applied to micropulse lidar data. In (a), the raw data shows evident cirrus during the night (low noise) and careful inspections shows that the layer persists into the day as the solar noise causes the background signal to increase. The SEM uses the statistics of these profiles to effectively increase the separation between signal and noise. In (b) the quantity p_{eff} is plotted. The light gray areas show $p_{eff} < -30.$, the dark gray areas show $-30. < p_{eff} < -20.$, and the medium gray areas show $p_{eff} > -20.$

can be expressed $p_i = \dfrac{1}{\sigma_n \sqrt{2\pi}} exp\left(-\dfrac{1}{2\sigma_n^2}\left(\overline{P_r} - P_{n,jk}\right)^2\right)$ where $\overline{P_r}$ is the mean signal in the data window. Since a low value of p could arise due to significant signal anywhere in the data window, we assign p to all the resolution volumes in the data window. A value p_i is then calculated at each resolution volume for the data windows associated with it and the effective value of p (p_{eff}) for that volume is taken as $p_{eff} = \sum_i log(p_i)$ for the $i = m \times n$ times it has been examined in conjunction with its nearest neighbors. In the case of a weakly reflective but spatially persistent hydrometeor layer p_{eff} becomes substantially negative for the affected range gates. Figure1 demonstrates an example of this algorithm applied to lidar data. We present this particular example to highlight the ability of the statistical approach to effectively separate the signal from the noise. In figure 1 we see that the cirrus observed during the night (06-09 UTC) could be easily identified with a thresholding algorithm while cirrus observed during the day are much more difficult to identify because their backscattered signal is very close to the noise threshold. The statistical algorithm identifies those portions near 10 km that are temporally persistent and even identifies areas of cloudiness near 7 km that are not immediately obvious by a cursory visual inspection. In figure 1b, the lighter colored regions of the cloud layer are those portions where $p_{eff} < -30$. The darker gray areas surrounding the light shaded regions are somewhat ambiguous areas where $p_{eff} < -20$.

48 BIT CLOUD MASK FILE SPECIFICATION		
BIT FIELD	DESCRIPTION KEY	RESULT
0	Cloud Mask Flag	0 = not determined
		1 = determined
1-2	Unobstructed FOV Quality Flag	00 = cloudy
		01 = uncertain clear
		10 = probably clear
		11 = confident clear
PROCESSING PATH FLAGS		
3	Day / Night Flag	0 = Night / 1 = Day
4	Sun glint Flag	0 = Yes / 1 = No
5	Snow / Ice Background Flag	0 = Yes / 1 = No
6-7	Land / Water Flag	00 = Water
		01 = Coastal
		10 = Desert
		11 = Land
ADDITIONAL INFORMATION		
8	Non-cloud obstruction Flag (heavy aerosol)	0 = Yes / 1 = No
9	Thin Cirrus Detected (near infrared)	0 = Yes / 1 = No
10	Shadow Found	0 = Yes / 1 = No
11	Thin Cirrus Detected (infrared)	0 = Yes / 1 = No
12	Spare (Cloud adjacency)	(post launch)
1-km CLOUD FLAGS		
13	Cloud Flag - simple IR Threshold Test	0 = Yes / 1 = No
14	High Cloud Flag - CO_2 Threshold Test	0 = Yes / 1 = No
15	High Cloud Flag - 6.7 μm Test	0 = Yes / 1 = No
16	High Cloud Flag - 1.38 μm Test	0 = Yes / 1 = No
17	High Cloud Flag - 3.9-12 μm Test	0 = Yes / 1 = No
18	Cloud Flag - IR Temperature Difference	0 = Yes / 1 = No
19	Cloud Flag - 3.9-11 μm Test	0 = Yes / 1 = No
20	Cloud Flag - Visible Reflectance Test	0 = Yes / 1 = No
21	Cloud Flag - Visible Ratio Test	0 = Yes / 1 = No
22	Cloud Flag - Near IR Reflectance Test	0 = Yes / 1 = No
23	Cloud Flag - 3.7-3.9 μm Test	0 = Yes / 1 = No
ADDITIONAL TESTS		
24	Cloud Flag - Temporal Consistency	0 = Yes / 1 = No
25	Cloud Flag - Spatial Variability	0 = Yes / 1 = No
26-31	Spares	
250-m CLOUD FLAG - VISIBLE TESTS		
32	Element(1,1)	0 = Yes / 1 = No
33	Element(1,2)	0 = Yes / 1 = No
34	Element(1,3)	0 = Yes / 1 = No
35	Element(1,4)	0 = Yes / 1 = No
36	Element(2,1)	0 = Yes / 1 = No
37	Element(2,2)	0 = Yes / 1 = No
38	Element(2,3)	0 = Yes / 1 = No
39	Element(2,4)	0 = Yes / 1 = No
40	Element(3,1)	0 = Yes / 1 = No
41	Element(3,2)	0 = Yes / 1 = No
42	Element(3,3)	0 = Yes / 1 = No
43	Element(3,4)	0 = Yes / 1 = No
44	Element(4,1)	0 = Yes / 1 = No
45	Element(4,2)	0 = Yes / 1 = No
46	Element(4,3)	0 = Yes / 1 = No
47	Element(4,4)	0 = Yes / 1 = No

Table 1. Bitwise description of the elements of the MODIS cloud mask. (adapted from Ackerman et al., 1998)

The threshold value p_{thresh} needs to be carefully tuned to maximize the correct identification of weakly reflective returns while minimizing the occurrence of false alarms. Like most thresholds values there is some amount of arbitrariness associated with p_{thresh}. We are continuing working with the CloudSat test data set to attempt to establish values for p_{thresh}, and we will continue that work during the initial post launch phase of the mission. Our current approach is based on examining many years of cloud

cloud-masked MMCR data from all the DOE ARM sites. The MMCR unmasked returned power is averaged vertically and temporally to simulate the CloudSat resolution and noise is added to decrease the sensitivity of the MMCR and simulate the mixer noise estimated for the CPR. The SEM algorithm is implemented on the simulated CloudSat data and the value of p_{eff} at each range gate is compared to the full resolution cloud masked MMCR data. The fraction of times that a CloudSat resolution volume with a particular value of p_{eff} contains hydrometeors as observed by the cloud-masked MMCR data is defined as $Q_h(p_{eff})$. The quantity $Q_h(p_{eff})$ is then used as an objective measure of the likelihood that a particular value of p_{eff} if used as p_{thresh} will correctly identify the occurrence of hydrometeor in the layer. A value of 1- $Q_h(p_{eff})$ identifies the likelihood of that value of p_{eff} if used as p_{thresh} resulting in false alarms.

2.2 SEM-MODIS Mask Intercomparison

CloudSat is expected to orbit within several degrees and approximately 5 seconds behind the EOS PM (Aqua) satellite ground track. Aqua hosts a number of platforms that will add substantially to the information content of the CPR profile. The majority of this synergistic association between the CPR data and the Aqua data streams will be explored in a research mode during and after the flight phase of the CloudSat project. However, data from one these instruments (MODIS) will be acquired and ingested into the operational CloudSat processing stream. We will incorporate the MODIS cloud mask product (MOD35; Ackerman et al, 1998) as a quality/confidence check of the CloudSat GeoProf output.

MODIS cloudmask data will be available at the native 1 km (day and night) and 250m (daytime only) horizontal resolutions in an across track swath along the CloudSat ground track. Each data point is provided in the form of a 48 bit word (Table 1) for each 1km MODIS pixel. Details of this product can be found in Ackerman et al. (1998) and Ackerman et al. (1997). Table 1 provides a description of the information contained in the bitwise elements of the 48 bit word. Given the nominal CloudSat footprint of 1.4 km across by 2.5 km along track, several MODIS 1 km pixels can be examined to determine the likelihood that the CloudSat footprint is only partially filled with hydrometeors. This determination will be important to establishing the validity of the radar reflectivity factor reported by the GeoProf algorithm and will provide information that is critical to various level 2 processing algorithms that will attempt to determine the microphysical and radiative properties of hydrometeor layers. These algorithms often rely on an assumption that the backscatter cross section per unit volume is due to a reasonably uniform distribution of hydrometeors within that volume.

We must first determine if the hydrometeor vertical characteristics identified by the SEM and the hydrometeor field observed by MODIS are reasonably similar. It is understood that some fraction of the hydrometeor-filled resolution volumes sampled by CloudSat will have a reflectivity below the minimum detectable signal of the CPR and will go undetected. Studies suggest that these clouds will be composed of primarily near-tropopause cirrus and liquid phase mid-level and boundary layer clouds. Stephens et al (Stephens et al., 2001) show that this characteristic of the CloudSat data does not detract from the main mission of the project − namely to characterize the radiative heating of the atmospheric column. However, it will be helpful to identify which CPR columns appear to suggest significantly different cloud characteristics from that reported in the MODIS cloud mask product.
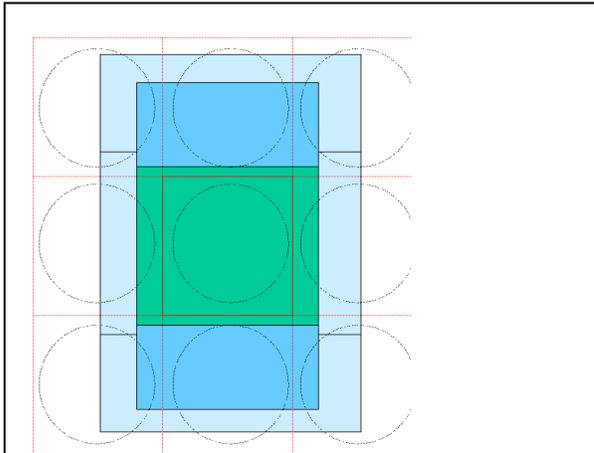

Figure 2. Schematic of the CloudSat-modis pixel configuration. The green rectangular area represents the 1.1 km region that will be most heavily weighted in the CloudSat CPR profile. The darker blue region will be less heavily weighted. The light green area represents the outer region that the CPR observational region due to pointing uncertainty. The grid square and circles represent the MODIS

The algorithm to compare the MODIS cloud mask and the CPR data will begin with a check of the status of the MODIS cloud mask and processing path used by the MODIS mask algorithm for the 15 1 km MODIS pixels nearest to the CPR profile in question. A weighting will be assigned to each pixel based on its location relative to the CloudSat footprint and the likelihood the pixel is within the CPR footprint. The schematic in Figure 2 illustrates the geometry of the problem accounting for the pointing uncertainty of the CPR of ~500 m. Once the pixel weighting is determined, bit 0 of each MODIS pixel will be examined to ensure that the MODIS mask has been implemented and the processing path for that pixel will be determined by examining bits 3-7 (see Table 1). The processing path bits identify which of the spectral tests are applicable. Bit 8 will also be examined to ensure that heavy aerosol (smoke or dust) was not present to significantly contaminate the visible channel radiances. By examining the spectral tests for each of the relevant MODIS pixels it will be possible to develop a broad characterization of the CloudSat scene. The level of detail that we can attain with this characterization will depend largely on the processing path taken by the MODIS cloudmask algorithm (Table 2). The processing path depends on the time of day and the surface ecosystem. The cloud characterization that we derive from the results of the cloud mask is limited to the following: 1) very thin high cloud, 2) thin high cloud, 3) thick high cloud, 4) high cloud, 5) mid level clouds, 6) low clouds, 7) non-high cloud. Table 3 shows which bits will be examined to determine a pixel characterization. In general, we will best be able to characterize the CloudSat scene in daytime over the unfrozen oceans because of the consistently dark and uniform background (when not in sunglint regions − bit 4). In general, scenes over nighttime land

		Day Ocean	Night Ocean	Day Land	Night Land	Polar Day (snow)	Polar Night (snow)	Coast Day	Coast Night	Desert Day	Desert Night
BT_{11}	(Bit 13)	✓	✓								
$BT_{13.9}$	(Bit 14)	✓	✓	✓	✓	✓	✓	✓	✓	✓	✓
$BT_{6.7}$	(Bit 15)	✓	✓	✓	✓	✓	✓	✓	✓	✓	✓
$R_{1.38}$	(Bit 16)	✓		✓		✓		✓		✓	
$BT_{3.7} - BT_{12}$	(Bit 17)				✓		✓				✓
BT_{8-11} & BT_{11-12}	(Bit 18)	✓	✓	✓	✓			✓	✓	✓	✓
$BT_{3.7} - BT_{11}$	(Bit 19)	✓	✓	✓	✓	✓	✓	✓	✓	✓	✓
$R_{.66}$ or $R_{.87}$	(Bit 20)	✓		✓				✓			
$R_{.87}/R_{0.66}$	(Bit 21)	✓		✓							
$R_{.935}/R_{.87}$	(Bit 22)	✓		✓			✓	✓			
$BT_{3.7} - BT_{3.9}$	(Bit 23)	✓		✓				✓		✓	
Temp Consis	(Bit 25)	✓	✓								✓
Spatial Variability	(Bit 25)	✓	✓								

Table 2. Modis cloudmask algorithm processing paths. The checks indicate which spectral tests are applied to a given ecosystem. Adapted from Ackerman et al., 1998.

will be difficult to characterize accurately due to the lack of a consistent IR background. Snow covered and other bright surfaces are also difficult to gauge accurately under many circumstances. These include desert, coastal, and mountainous regions.

High clouds are defined as having a cloud top pressure less than 500 mb and the designations of very thin, thin, and thick depend on the results of the spectral tests listed in Table 3. Taken together, these tests correspond in a broad sense to the optical thickness of the high layer. The thin and thick designations will be determined based on the results of IR and visible reflectance threshold tests reported in bits 13 and 20-22. For a high cloud to be classified as thick, we will require that it be thick enough to appear cold in the infrared window spectral region and be identifiable in at least one of the visible reflectance tests for daytime data. The most thorough test for thin and thick high clouds are possible over warm ocean surfaces due to the relative reliability of the IR threshold tests. Over daytime land the visible reflectance tests will be used. Along other processing paths it will not be possible to determine a thickness designation for high clouds using the MODIS cloud mask, thus the simple designation of high cloud will be used in the case that certain other bit tests suggest clouds above 500 mb. Bit 14, for instance, should be a reliable indicator of the presence of high clouds along any of the processing paths. The designation of very thin high clouds will be applied when the near IR spectral test (bit 9) suggests clouds but no other high cloud test is positive.

Thick mid level clouds will be discernable under some circumstances. Over the ocean, when bit 14 does not identify clouds then we can assume that the cloud top pressure is higher than 500 mb. However, if the cloud appears cold as reported by the IR threshold test (bit 13) and the underlying ocean is warm (as determined with meteorological data) we can reasonably suspect an optically thick cloud whose top is colder than freezing. During daytime, this classification will be aided by the use of visible reflectance tests since these cloud layers should be reflective in the visible and near infrared. Low-level clouds will be identified through various tests most of which are not implemented during the night. Thus we will often be unable to discriminate between clouds with tops in the middle and lower troposphere. These cases will be designated as non-high clouds.

Table 3. MODIS pixel cloudiness characterizations using cloudmask bit tests. Assumes the cloudmask has been implemented according to bit 0 and that the pixel has been classified as cloudy or low confidence clear by bits 1 and 2. The blacked out regions in this table denote cloud types in certain ecosystems that cannot be evaluated with confidence. More detailed flow charts are shown in Appendix A.

Designation	Numerical Designation	MODIS Bit Value	Bits Examined for specific ecosystems							
			Day Ocean	Night Ocean	Day Land	Night Land	Polar Day (snow)	Polar Night (snow)	Desert Day	Desert Night
Unclassifiable	9		Bit tests provide contradictory results for a cloudy pixel							
No Test	0	0	0							
Clear	1	10,11	1 and 2							
High Cloud	2	0	14	14	14	14	14	14	14	14
		1								
High Cloud, Very Thin	3	0	9	17	9	17	9	17	9	17
		1	13, 16	13	16	14	14	14	14	14
High Cloud, Thin	4	0	14, 16, 9	14, 11, 17	14, 16, 9					
		1	13, 22	13	22					
High Cloud, Thick	5	0	14, 16, 9, 13, 20, 21	14, 13	14, 16, 9, 20, 21					
		1								
Non High Cloud	6	0	13, 20, 21, 22, 19, 23	13, 18	20, 21, 22, 19, 23	18	22, 19		18, 23	18
		1	14, 9	14, 11	14, 9, 11, 16	14	14, 9		14, 9, 16	14, 11
Mid Cloud, Thick	7	0	13, 20, 21, 22, 19, 23	13						
		1	14, 9, 16	14, 16						
Low Cloud	8	0	20, 21, 22, 19, 23	18						
		1	13, 14, 9, 16	13, 14, 16						

Seemingly disparate possibilities will also be encountered and will be listed as unclassifiable. For instance, the thin cirrus identified by only the near IR threshold test (bit 9 or bit 16) will often be so thin that other tests will not be biased by its presence. Thus it will not be uncommon to encounter pixels that contain low-level clouds identifiable in the solar reflectance tests and thin cirrus. This situation is especially likely in the tropics and subtropics. Other possibilities include thin high clouds as observed by bit 14 with other low cloud indicators such as bits 19 or 18. These circumstances will often be indicative of multi-layered situations that can be verified in some circumstances with CloudSat data. Once the MODIS pixels composing a CloudSat footprint are characterized, the overall classification will be determined as a weighted mean of the various pixel types where thin and thick high cloud will be considered to compose a single type. To facilitate comparison between the CloudSat and Modis observations, the masked CPR data will be classified similarly according to Table 4.

Table 4. CPR echo top characterization

Cloud Classification	Numerical Designation	Definition
No Determination	0	
Clear Profile	1	No hydrometeor layers found in CPR profile
High Cloud	2	Echo top pressure less than 500 mb.
Mid Level cloud	3	Echo top pressure greater than 500 mb and echo top temperature colder than 273.
Low Level cloud	4	Echo top pressure greater than 500 mb and echo top temperature warmer than 273.
Multi Layer	5	Distinct combinations of above types

A variability classification will also be assigned to the scene using the 1km classified Modis pixels that compose the CloudSat footprint and immediately adjacent region (6-9 pixels) and will be labeled according to the criteria in Table 4.

Table 5. CloudSat Scene Variability Designation

CloudSat Scene Variability	Numerical Designation	Fraction of MODIS pixels in the vicinity of the CloudSat footprint with same cloud type
No Determination	0	
Highly Uniform	1	≥ 0.9
Uniform	2	≥ 0.75
Weakly Variable	3	$0.5 - 0.75$
Variable	4	≤ 0.5
Highly Variable	5	≤ 0.25

Additionally, during daylight regions over ocean (not including sun glint), bits 32-47 record the results of simple visible threshold tests applied to the central 16 250m pixels of a 1km MODIS pixel. Since only two channels are used to establish the presence of cloudiness in the 250m pixels, the uncertainty in each pixel is expected to be larger than the associated 1km value. However, our goal is to estimate the degree of scene uniformity. The overall cloud fraction provided by these tests will be useful for establishing this uniformity. This fractional cloud cover will, therefore, be calculated as a weighted mean of the MODIS pixels composing the field of view and recorded in tenths of coverage.

Our primary goal with this comparison is to establish the overall complimentarity of the combined data stream. In cases where we can establish that the CloudSat and MODIS representations are similar in regions with uniform cloudiness, then higher order algorithms can be implemented with confidence. In the opposite case, when the MODIS and CloudSat representations are different significantly, we will know that caution will need to be exercised in the application and interpretation of retrieval. Ultimately, this

comparison will improve our understanding of both data sets since much more detail will be available than either could provide alone.

2.3 Validation

Actual Comparison between CloudSat and MODIS data will obviously not be possible until after both instruments are generating data in orbit. We developed a library of cloud cases from several ground validation sites. These cases include Terra MODIS scenes, millimeter radar and other ancillary data that allow us to closely simulate the data streams that will be available during the CloudSat mission. This library of cases covers a wide range of cloud types over multiple ecosystems. This library includes 193 real cases of millimeter radar data from three ARM sites (57 TWPC2 cases, 63 SGP case, 73 NSA cases) and the corresponding MODIS data (Appendix C). It includes clear sky, high clouds (very thin, thin, thick), middle clouds, low clouds and multi-layer clouds (Table 6). Since MODIS data from Aqua are not yet available and the MODIS algorithms continue to evolve, evaluation and refinement of all aspects of the GEOPROF algorithm will continue until launch.

Table 6. Test data set

	TWPC2 (day)	TWPC2 (night)	SGP (day)	SGP (night)	NSA (day)	NSA (night)
Clear	5	5	5	5	5	5
High cloud	5	4	5	2	4	3
High cloud, very thin	1	4	5	6	2	5
High cloud, thin	2	2	5	2		4
High cloud, thick	4	4	5	5	2	5
Middle cloud	3	3	3	3	4	10
Low cloud	6	1	4	2	5	8
Multi-layer cloud	4	5	4	2	5	6

3. Algorithm Inputs

3.1. CloudSat

3.1.1. CloudSat Level 1B CPR Science Data

The CPR Level 1 B (Li and Durden, 2001) is the main input for the GEOPROF Algorithm. 2B-GEOPROF algorithm requires the following inputs from the Level 1B CPR Science Data are (see Level 1B CPR Process Description and Interface Control Document). Spacecraft latitude and longitude are used to locate the position of satellite. Range bin sizes, Range to first bin, and Surface bin number are used to locate the height of resolution volumes. Received echo power is used as input to the SEM algorithm and

for calculation of radar reflectivity. Radar transmission power, wavelength, and radar calibration coefficients are also needed when calculating radar reflectivity.

- Spacecraft latitude
- Spacecraft longitude
- Spacecraft altitude
- Range bin sizes
- Range to first bin
- Surface bin number
- Wave length
- CPR radar calibration coefficients
- Radar transmission power
- Received echo power

3.1.2. CloudSat Level 1A Auxiliary Data

Level 2 GEOPROF processing requires the following data:

– Land/Sea Flag
– Altitude of Surface

3.2.   Ancillary (Non-CloudSat)

3.2.1. MODIS cloud mask data

The MODIS cloud mask data will be used for the comparison of the geometrical profile algorithm with the MODIS cloud mask spectral tests.

– MODIS latitude
– MODIS longitude
– 48 bit MODIS mask data in a swath along the CLOUDSAT ground track

3.2.2. ECMWF

Meteorological data interpolated temporally and spatially to the CLOUDSAT range resolution volumes are needed to aid in the comparison of MODIS mask data with CLOUDSAT profile data. Temperature and pressure profiles are required for the calculation of CPR echo top characterization (see Table 4).

– Temperature profile
– Atmosphere pressure profile

3.3. Control and Calibration

This algorithm does not require control and calibration data.

4. *Algorithm Summary*

4.1. *The Significant Echo Mask Algorithm*

The CPR records range-resolved profiles of backscattered power. The SEM algorithm is designed for identification of hydrometeor echo.

> *Read Level 1 B data granule*
> *Put in loop over granule*
> *Use Level 1 B Data*
>
> *If $P_r \geq (P_n + (3\sigma_n))$ then*
>   *cloud was detected*
>   *set cloud_mask = 1;*
> *end-if*
>
> *while $P_r \leq (P_n + (3\sigma_n)))$ then*
>   *consider spatial and vertical continuity*
>   *calculate Gaussian probability that p_r is noise in 3×3 box*
>   *calculate p_{eff} --- the effective value of p*
>   *$p_{eff} = \Sigma(log(p))$*
>   *calculate quality assurance Q_A*
>
>   *if ($p_{eff} \geq p_{thresh}$)then*
>   *cloud was detected*
>   *cloud_mask = 1*
>   *else*
>   *no cloud*
>   *cloud_mask = 0*
>   *end-if*
> *end-while*
>
> *$P_r = P_r \times cloud\_mask$*
> *calculate reflectivity*
>
> *output radar reflectivity*
> *output CPR cloud mask*
> *output quality assurance Q_A* (under development)

4.2 *SEM-MODIS Mask Intercomparison*

To summarize, the steps in Intercomparison of SEM and MODIS are:

Read MODIS cloud mask and MODIS navigation data
Read ECMWF data

Identify appropriate MODIS pixels
Determine pixel weighting to CLOUDSAT footprint

Determining MODIS cloud classification
    If (bit 0 equals 0) then
        No MODIS determination is needed
    Else
    If (bit 1, 2 equal 10 or bit 1, 2 equal 11) then
        Clear atmosphere
    Else
        Determining MODIS cloud classification using the flow charts in
        Appendix A.
            Check the surface ecosystems
            Check the bits to determining cloud classification
    End-if

Determining CPR cloud classification (Table 4)

Calculate CloudSat scene variability (Table 5)

Calculate cloud fraction with 250m pixels when possible

Output MODIS cloud classification
Output CPR echo top characterization
Output CloudSat scene variability
Output MODIS 250m cloud fraction

5. Data Product Output Format

5.1. Format Overview

The CPR Level 2 GEOPROF Product will produce an estimate of the radar reflectivity factor and cloud mask.

The format chosen for CPR Level 2 GEOPROF data is similar to that for CPR Level 1 B data. The format consists of metadata, which describes the data characteristics, and swath data, which includes the radar reflectivity factor, cloud mask and other information. The following schematic illustrates how GEOPROF data is formatted using HDF EOS. The variable nray is the number of radar profiles (frames, rays) in a granule. Each block is a 0.16 s average of radar data.

Table 6. CPR Level 2 GEOPROF HDF-EOS Data Structure

Data Granule	CloudSat Metadata			TBD	
	CPR Metadata			TBD	
	Swath Data	Time		Table: nray 10 bytes	
		Geolocation		$2 \times$ nray 4-byte float	
		SEM	Radar Reflectivity	$125 \times$ nray 2-byte integer	
			Quality assurance Q_A	$125 \times$ nray 1 byte integer	
			CPR Cloud Mask	$125 \times$ nray 1 byte integer	
		SEM-MODIS	MODIS scene characterizations (Table 3)	1 byte	nray
			CPR echo top characterizations (Table 4)	1 byte	
			MODIS scene variability (Table 5)	1 byte	
			MODIS 250m cloud fraction	1 byte	

5.2. CPR Level 2 GEOPROF HDF-EOS Data Contents

The contents of the metadata are still TBD and so the sizes are also TBD.

❑ **CloudSat Metadata** (Attribute, Size TBD)

TBD by CIRA

❑ **CPR Metadata** (Attribute, Size TBD)

TBD by CIRA

❑ **Time** (Vdata data, array size nray, record size 10 byte):

Time is determined based on VTCW time. See Table 2 of Li and Durden (2001) for data format.

❑ **Geolocation** (SDS, array size 2 × nray, 4-byte float):

As documented in Li and Durden (2001), geolocation is defined as the Earth location of the center of the IFOV at the altitude of the Earth ellipsoid. The first dimension is latitude and longitude, in that order. The next dimension is ray number. Values are represented as floating point decimal degrees. Off earth is represented as less than or equal to -9999.9. Latitude is positive north, negative south. Longitude is positive east, negative west. A point on the 180th meridian is assigned to the western hemisphere.

❑ **SEM product**

   ▪ **Radar Reflectivity** (SDS, array size 125 × nray, 2-byte integer)

Radar reflectivity factor Z_e is calculated with the echo power (P_r) and other input data as described in Level 1B CPR Process Description and Interface Control Document (Li and Durden, 2001).

   ▪ **Quality assurance Q_A** (SDS, array size 125 × nray, 1-byte integer)

Quality assurance Q_A is the likelihood that a CloudSat resolution volume with a particular value of p_{eff} contains hydrometeors as compared to MMCR data.

   ▪ **CPR Cloud Mask** (SDS, array size 125 × nray, 1-byte integer)

Each CPR resolution volume is assigned 1 bit mask value:

   0 = No cloud detected
   1 = Cloud detected

❑ **SEM-MODIS product**

   ▪ **MODIS scene characterizations (SDS, 1-byte integer)**

This data includes MODIS pixel cloudiness characterizations using cloudmask bit tests. See Table 3 for a detailed specification.

   ▪ **CPR echo top characterizations (SDS, 1-byte integer)**

See Table 4 for the detail specification.

- **MODIS scene variability (SDS, 1-byte integer)**

MODIS scene variability includes the variability classification assigned to the CloudSat scene using the 1 km classified MODIS pixels that compose the CloudSat footprint and immediately adjacent region. See Table 5 for detail specification.

- **MODIS 250m cloud fraction (SDS, 1-byte integer)**

MODIS 250 m cloud fraction includes cloud fraction calculated with MODIS 250m pixels.

6. Operator Instructions

The Level 2 GEOPROF product processing software is integrated into the CloudSat Operational and Research Environment (CORE). It is called using the standard CORE procedure for calling modules to operate on data files. The output is in the form of an HDF-EOS structure in memory, which can be saved by CORE and passed on to other Level 2 processing.

For quality assessment purposes, quick look images of the significant echo mask algorithm is created that show the results of the SEM algorithm and the unmasked echo powers before the significant echo mask is created (Appendix B1, Figure 3). The orbit is divided into four even sections in the images. The upper panel is CLOUDSAT return echo power before the SEM mask is applied. The middle panel is CLOUDSAT radar reflectivity after the SEM mask is applied. Coherent regions of return different from the background noise apparent on the upper panel should be visible in the middle panel as significant echo return. The lower panel is MODIS unobstructed FOV quality flag (bit 1 and 2). The red, green, blue and black lines represent, respectively, cloudy, uncertain clear, probably clear and confidently clear. The CloudSat track follows the middle of the plot. By comparing the middle and lower panels, we are able to compare the coincidence between the measurements of CLOUDSAT and MODIS.

Statistics of CloudSat profiles and MODIS cloud classifications are generated for quality control of the SEM-MODIS algorithm. An ASCII file is created to save these statistics for each orbit. The file is written under directory "C:\Data\Devel\2B-GEOPROF\Output\". Description and a sample of the diagnostic statistics ASCII output are given in Appendix B2. Plots for the ASCII output are also made for quality assessment purposes. Description and a sample of the plots are given in Appendix B3.

7. CloudSat 2B GEOPROF Version R04 Quality Statement: May 2007

The primary purpose of the 2B GEOPROF product is to identify those levels in the vertical column sampled by CloudSat that contain significant radar echo from hydrometeors and to provide an estimate of the radar reflectivity factor for each of these volumes. Details on the GEOPROF algorithms and structure of the NetCDF output files are provided in the **Level 2 GEOPROF Product Process Description and Interface Control Document.**

http://www.cloudsat.cira.colostate.edu/dataICDlist.php?go=list&path=/2B-GEOPROF

Summary of changes from R03 to R04

An estimate of surface clutter (contained in 1B-CPR R04) is now subtracted from the return power in bins 2 through 5 above the surface. The original return power is kept in the surface bin, the bin 1 above the surface and all bins below the surface. See text below for more discussion.

There are four additional variables in the R04:

Clutter_reduction_flag

This flag has a value of 1, whenever an estimate of surface clutter has been subtracted from the measured return power (in bins 2 through 5 above the surface). It is zero, otherwise.

SurfaceHeightBin_fraction

This variable indicates the fractional location of the surface with in the pixel given by the variable "SurfaceHeightBin". This value is estimated in the clutter estimation processes. The altitude of the surface with respect to mean sea level is thus given by Height(SurfaceHeightBin) + RangeBinSize*SurfaceHeightBin_fraction.

This variable is real valued. Values less than -5 should not be used and indicate that the 2B GEOPROF code did consider the fraction to be valid.

MODIS_cloud_flag

This variable contains the MODIS summary cloud flag (bits 3 and 4 from MOD35) for the CloudSat column. Values are:

> 0 = Clear High Confidence
> 1 = Clear Low Confidence
> 2 = Cloudy Low Confidence
> 3 = Cloudy High Confidence

Note: the variable "MODIS_cloud_fraction" in 2B GEOPROF R03 and R04 is the fraction of VISIBLE pixels in the MODIS 250 m mask that are cloudy. This cloud fraction is only valid during the day and does not include cloud detection from at IR channels.

Sigma-Zero

This variable is a pass through from 1B-CPR. It is the estimated surface reflectance (in units of dBZ * 100).

Discussion of Product & Product Quality

The significant echo mask is stored under the variable name "CPR_Cloud_Mask", and contains a value between 0 and 40 for each range bin with values greater than 5 indicating the location of likely hydrometeors. Increasing values of the "CPR_Cloud_Mask" variable indicate a reduced probability of a false detection, as summarized in Table 1.

Mask Value	Meaning	% False Detections Goal	Estimated % False Detection via CALIPSO comparison
-9	Bad or missing radar data		
5	Significant return power but likely surface clutter		
6-10	Very weak echo (detected using along-track averaging)	< 50 %	44 %
20	Weak echo (detection may be artifact of spatial correlation)	< 16%	5 %
30	Good echo	< 2 %	4.3 %
40	Strong echo	< 0.2 %	0.6 %

Table 1 – Description of CloudSat cloud mask values, false detection rates, and percentage of false detections. The percent of false detection is given by 100 times the number of false detections divided by the total number of detections for the specified cloud mask value.

Users are cautioned that radar detections with cloud mask values between 6-10 contain large numbers of false detection. These possible detections represent hydrometeors whose radar-reflecivity is below the single column sensitivity limit of the radar (about – 30 dBZe), and have only been identified as a result of an aggressive along track averaging algorithm. For most applications, users should consider using cloud-mask values of 30 to 40, which are high-confidence detections.

In addition to the cloud mask, this product contains the radar reflectivity (i.e., the calibrated measured return power in units of dBZe = dB(mm^6/m^3)), an estimate of gaseous absorption loss of the observed reflectivity, and several quality indicator flags. Unlike typical weather radars, which operate at much longer wavelengths and are primarily designed to detect rain rather than clouds, the effect of water vapor on CloudSat observed reflectivity can be significant. Two-way attenuation from the surface to the satellite of more than 5 dBZ is not unusual in the tropics.

No estimate of loss in reflectivity due to absorption or scattering by hydrometeors is included in the GEOPROF, and users are cautioned that losses of 10 dB/km or higher are possible with large liquid water contents. At times, the CloudSat radar is fully attenuated, or attenuated to the point where multiple-scattering dominates the measured return power – though this is not common.

The cloud mask, reflectivity-field, and gaseous absorption are all provided on a height grid with 125 vertical range bins, where the CloudSat range bin closest to mean sea level has been placed in vertical bin 105. The location of the range bin that is closest to the actual surface location is also provided.

Overall, the most significant difficulty with the CloudSat data is that surface clutter effectively reduces the radar sensitivity near the surface. Figure 1, below, show the estimated radar return power during clear sky conditions. This is a typical result for an orbits colleted early in the mission. As a result of the surface contamination, all cloud mask detections below roughly the 99th percentile of the clear-sky return (dashed lines) are currently being set to a value of 5, to indicate there is return power above the radar noise floor but the signal is indistinguishable from surface clutter. While this conservative threshold should keep the false detection rate (by volume) below 1%, it also means that typically only rain and heavy drizzle can be detected in the third bin above the surface (~ 720 m) and moderate drizzle in the fourth bin (~ 860 m).

Starting with revision 04, we begun subtracting an estimate of the surface clutter from the total measured return power. We refer to this process as clutter rejection. Figure 2 shows the resulting clear-sky noise after clutter rejection. After clutter rejection, detection over ocean is improved with rain and heavy drizzle detectable at ~ 480 m and moderate drizzle at ~ 720 m. Clutter is reduced over land as well, but not as effectively.

Users are cautioned that clutter rejection (and cloud masking near the surface) is not very good over land regions that are not flat. The clutter rejection and cloud masking has been optimized for data collected after August 15, 2006 (starting with orbit 1595). The clutter rejection is being applied to all data (when valid), but cloud masking is based on pre-clutter rejection thresholds prior to orbit 1595 (figure 1).

The clutter rejection technique also estimates the position of the surface to a sub-range-bin scale, such that the position of the surface is given by SurfaceHeightBin + SurfaceHeightBin_fraction.

Finally, the CloudSat orbit follows closely the orbit of the AQUA satellite on which a number of advanced passive remote sensors observe the earth. The GEOPPROF data files include the Moderate-Resolution Imaging Spectroradiometer (MODIS) cloud fraction (from the visible 250 m MOD35 product) integrated over the CloudSat footprint, as well as a cloud scene classification (based on MOD35 cloud detection bit tests). Details of these parameters are given in the **Level 2 GEOPROF Product Process Description and Interface Control Document.** Starting with R04 there is also a MODIS cloud flag output, which provides the MODIS summary cloud test (bits 2 and 3 of standard MODS 35 product) under the CloudSat ground track.

Figure 1 - Estimate of the clear-sky observed return power. At the beginning of the CloudSat mission, the radar was unknowningly pointed 1.7 degrees off nadir. This was corrected starting with orbit 1023, and the radar pointed directly towards nadir. However, it was found that pointing directly at nadir increased the surface reflectance and the effect of surface clutter approximately 10 dB due to specular reflection. Thus, starting with orbit 1595 (August 15 at 20 UTC) the instrument was set to point 0.16 degrees of nadir. This angle put the specular reflection in the first antenna null and reduced the surface clutter to previous levels. Data from these time periods is referred to as epic "E" 00, 01, and 02 (given in each file name), respectively. Data shown here is "typical" for data in epic 00 and epic 02 before clutter rejection.
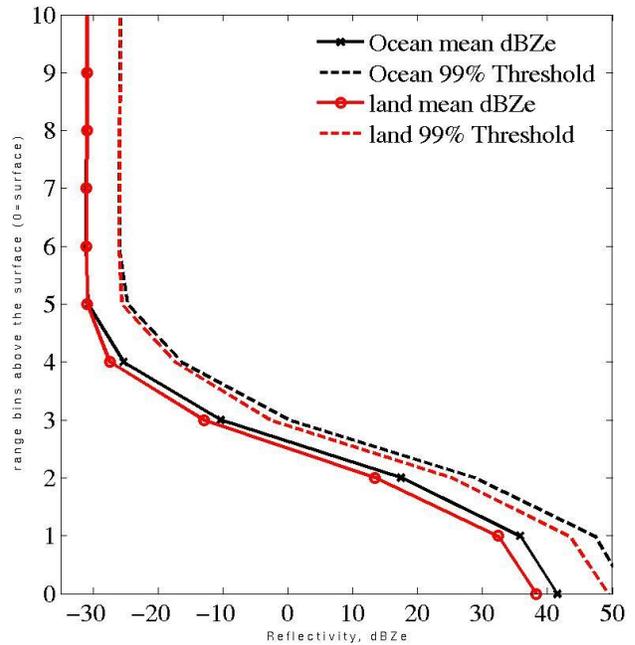
Figure 2 – Estimate of clear-sky return power AFTER application of clutter rejection. The clutter rejection is being applied in all epics, but is only optimal after orbit 1595 (August 15, 2006 20 UTC). Cloud masking prior to orbit 1595, continue to use conservative thresholds (as shown in figure 1). Cloud Mask starting with orbit 1595 use more aggressive thresholds.

23
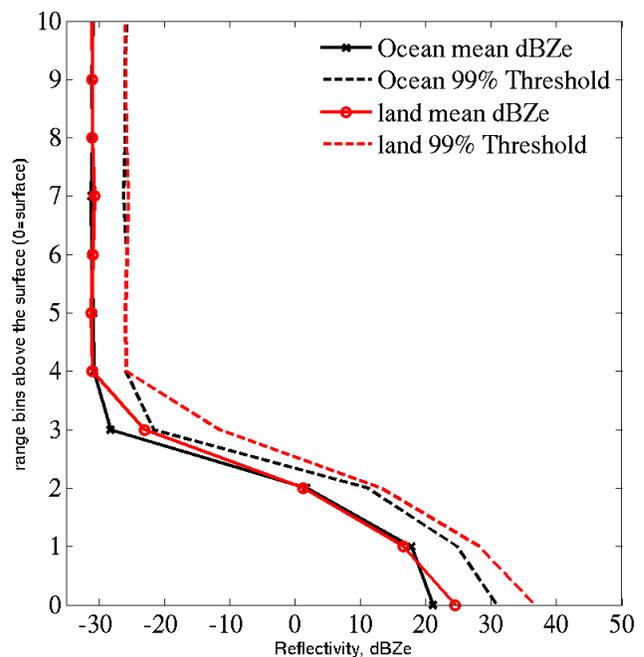
8. References

Ackerman, S. A., K. I. Strabala, W. P. Menzel, R. A. Frey, C. C. Moeller, L. E. Gumley, 1998: Discriminating clear sky from clouds with MODIS. *J. Geophys. Res.,* **103,** 32141-32157.

Clothiaux, E.E., G. G. Mace, T. P. Ackerman, T. J. Kane, J. D. Spinhirne, V. S. Scott, 1998: An Automated Algorithm for Detection of Hydrometeor Returns in Micropulse Lidar Data. *J. Atmos. and Oceanic Technol.,* **15,** 1035-1042,

Li, L. and S. Durden, 2001: Level 1 B CPR Process Description and Interface Control Document. Jet Propulsion Laboratory.

Stephens, G. A., D. Vane, and many others, 2001: The CloudSat mission and the EOS constellation: A new dimension to space-based observations of clouds and precipitation. Submitted to *Bull. Amer. Meteoro. Soc.*

9. Acronym List

SEM – Significant Echo Mask
MODIS – Moderate-Resolution Imaging Spectroradiometer

Appendix A. Flowcharts of MODIS pixel cloudiness characterizations

1. Flowchart of Ocean/Day
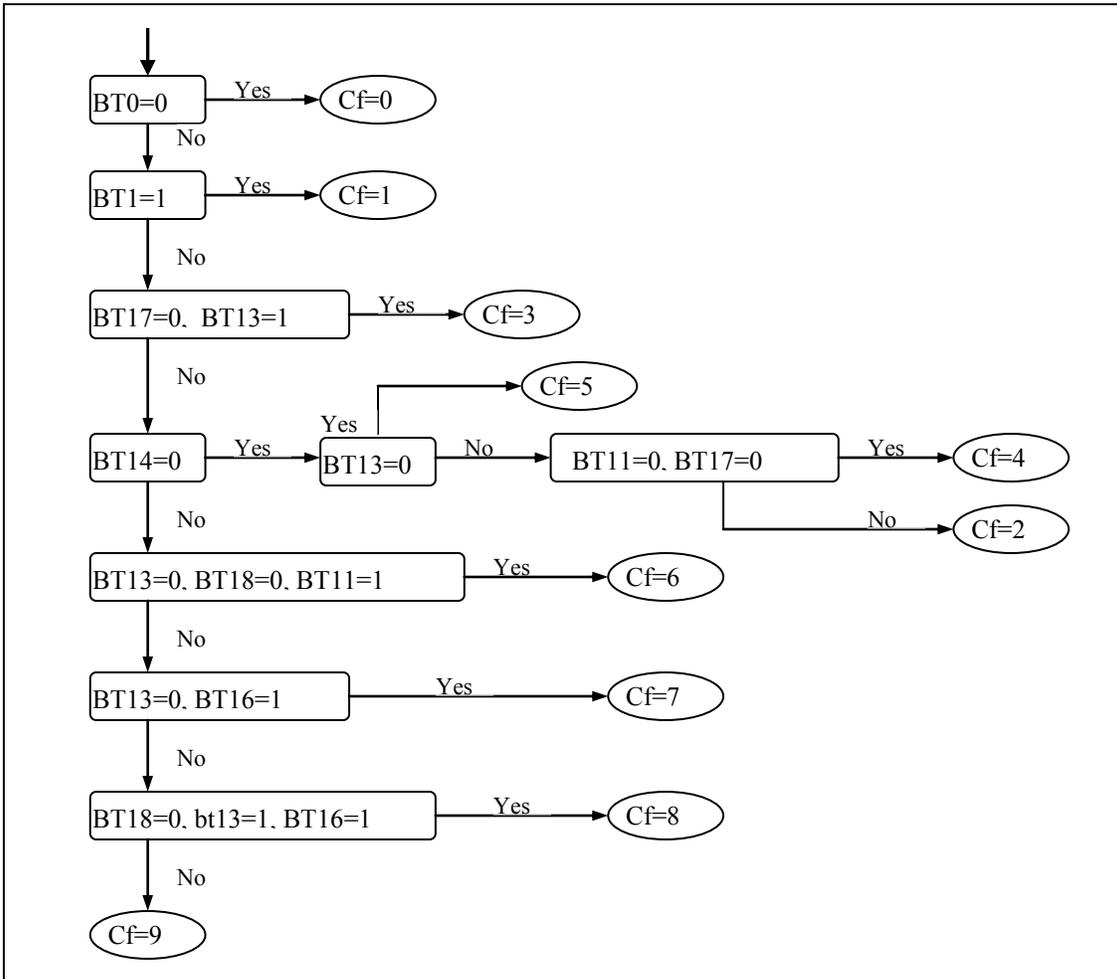
2. Flowchart of Ocean/Night
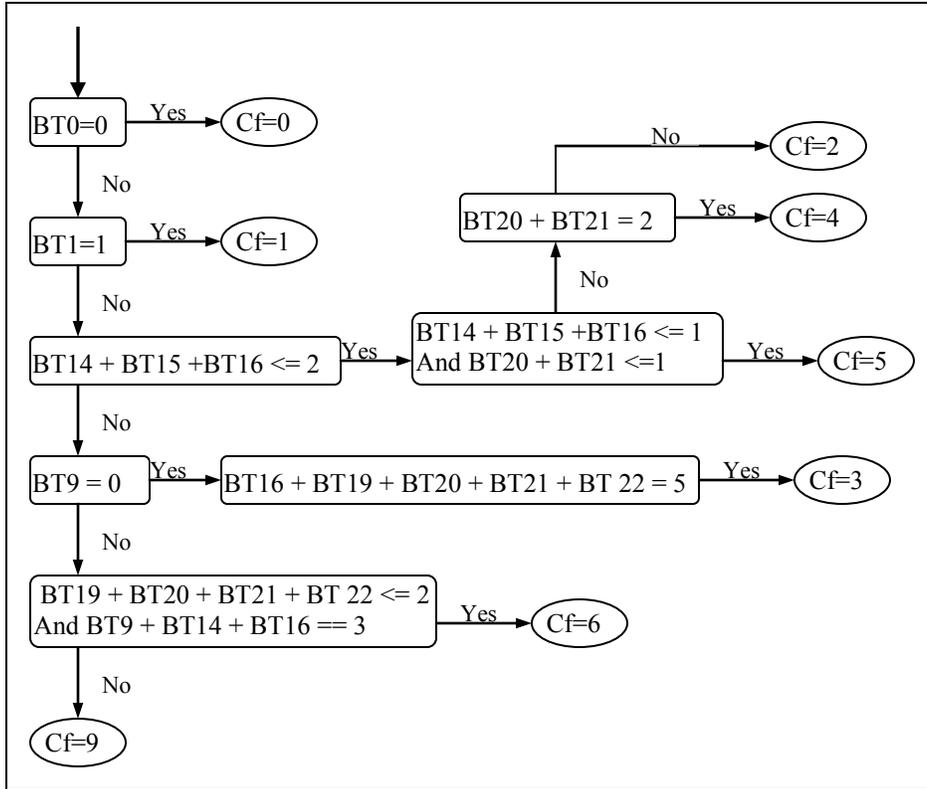
3. Flowchart of Land/Day
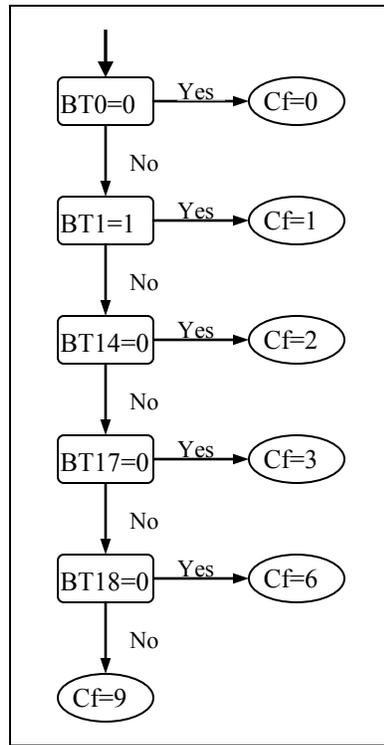
4. Flowchart of Land/Night
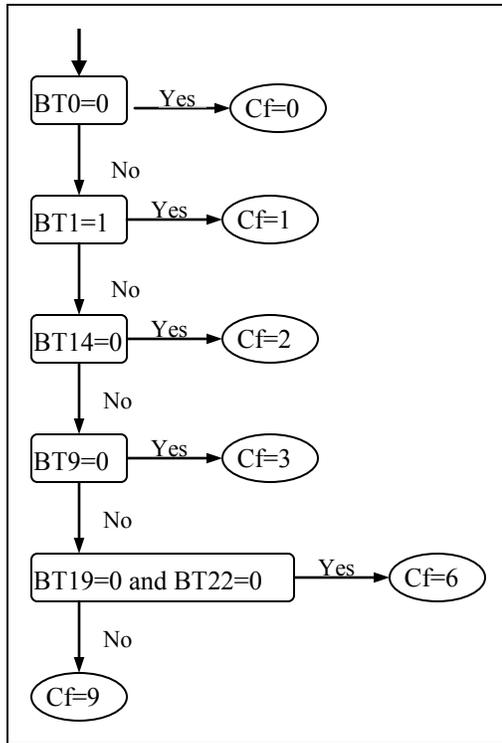
5. Flowchart of Polar/Day
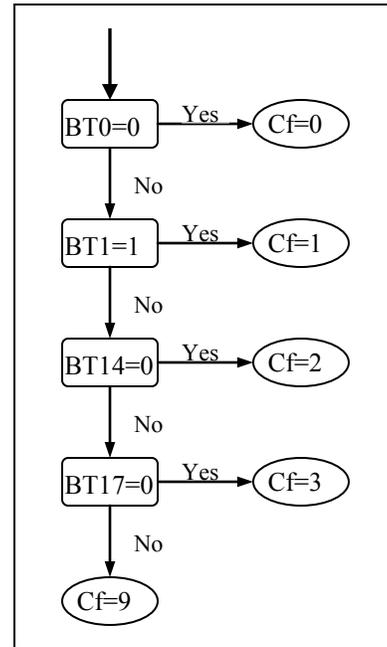
6. Flowchart of Polar/Night
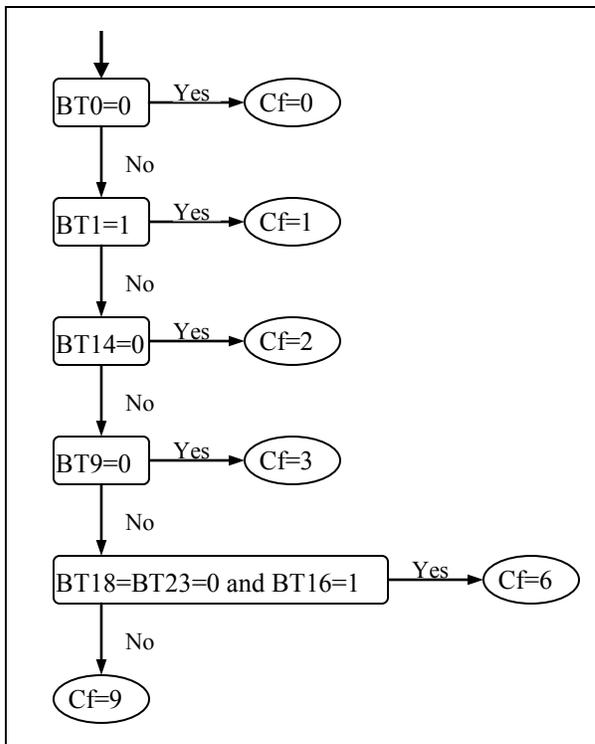
7. Flowchart of Desert/Day
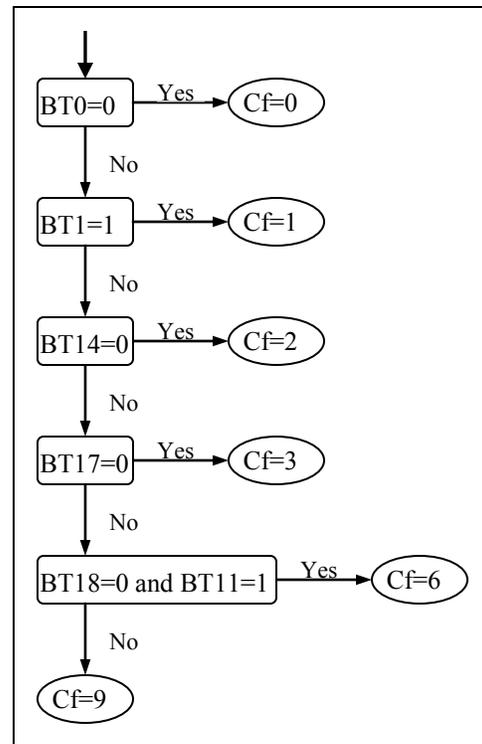
8. Flowchart of Desert/Night

Appendix B. Quality Assessment

B1. Plots of CLOUDSAT return echo power before the SEM mask, radar reflectivity after the SEM mask, and MODIS Unobstructed FOV Quality Flag for quality assessment purposes
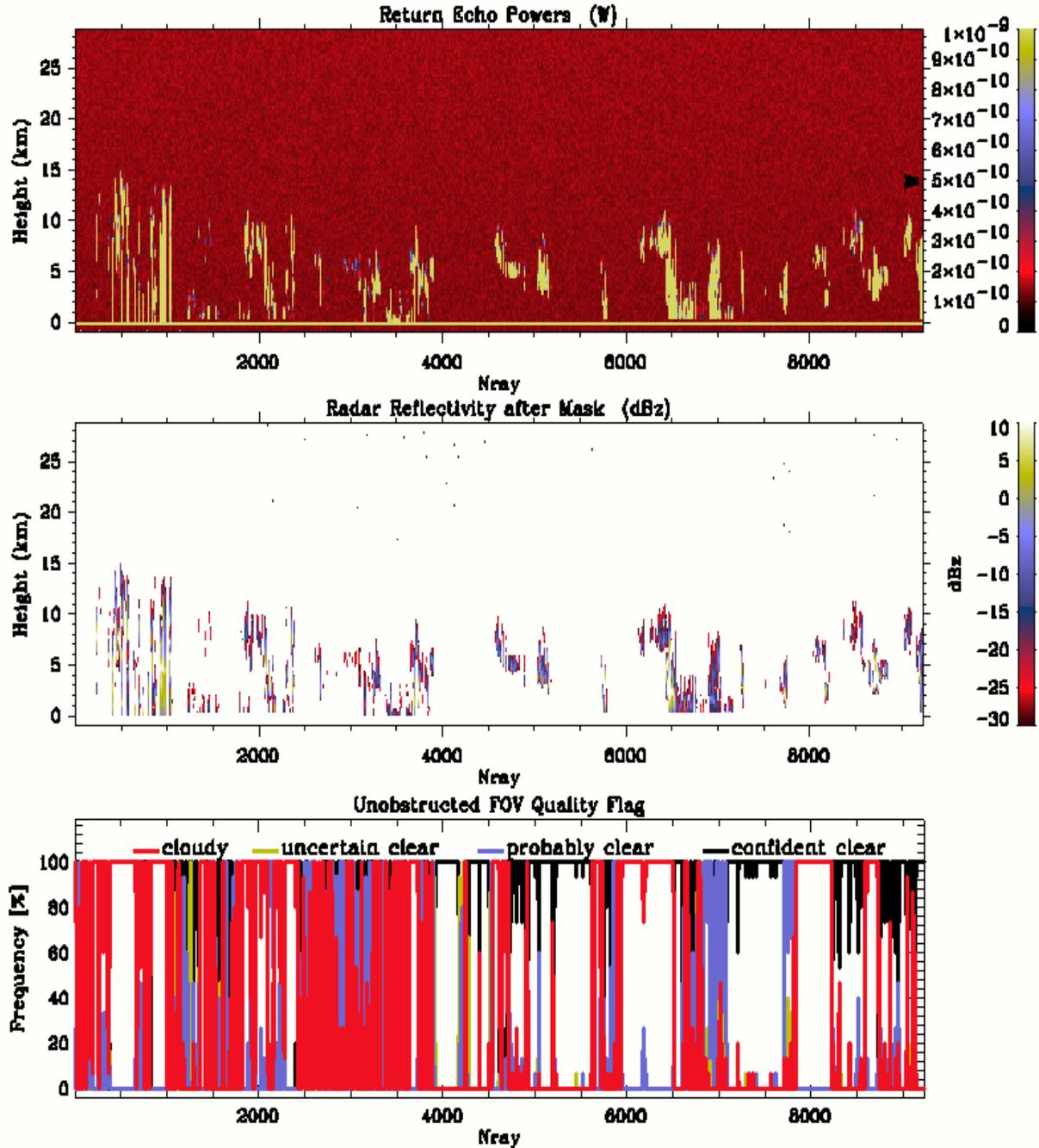
Figure 3(a). Return echo power before significant echo mask and radar reflectivity after mask (section 1).
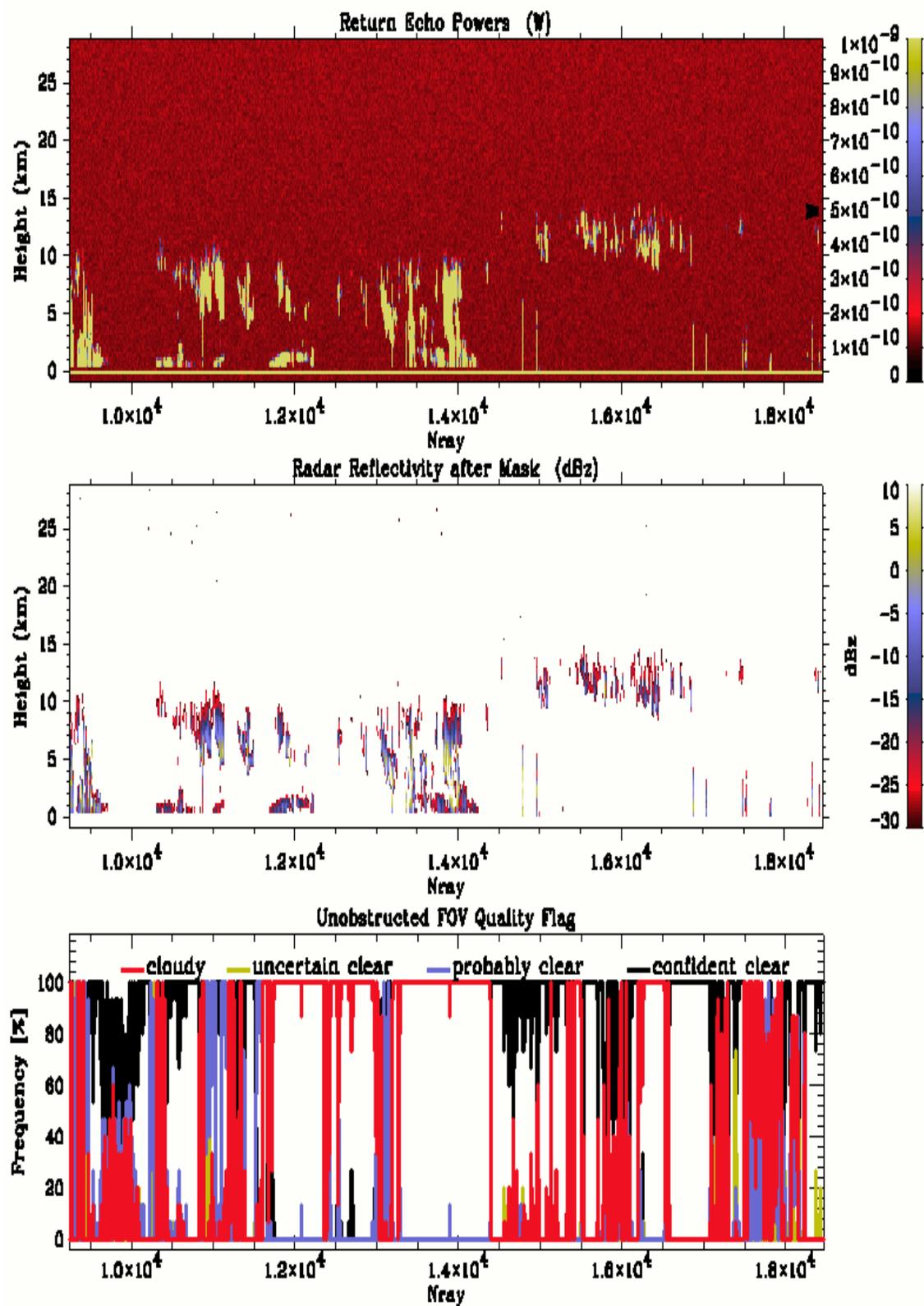
Figure 3(b). Return echo power before significant echo mask and radar reflectivity after mask (section 2).
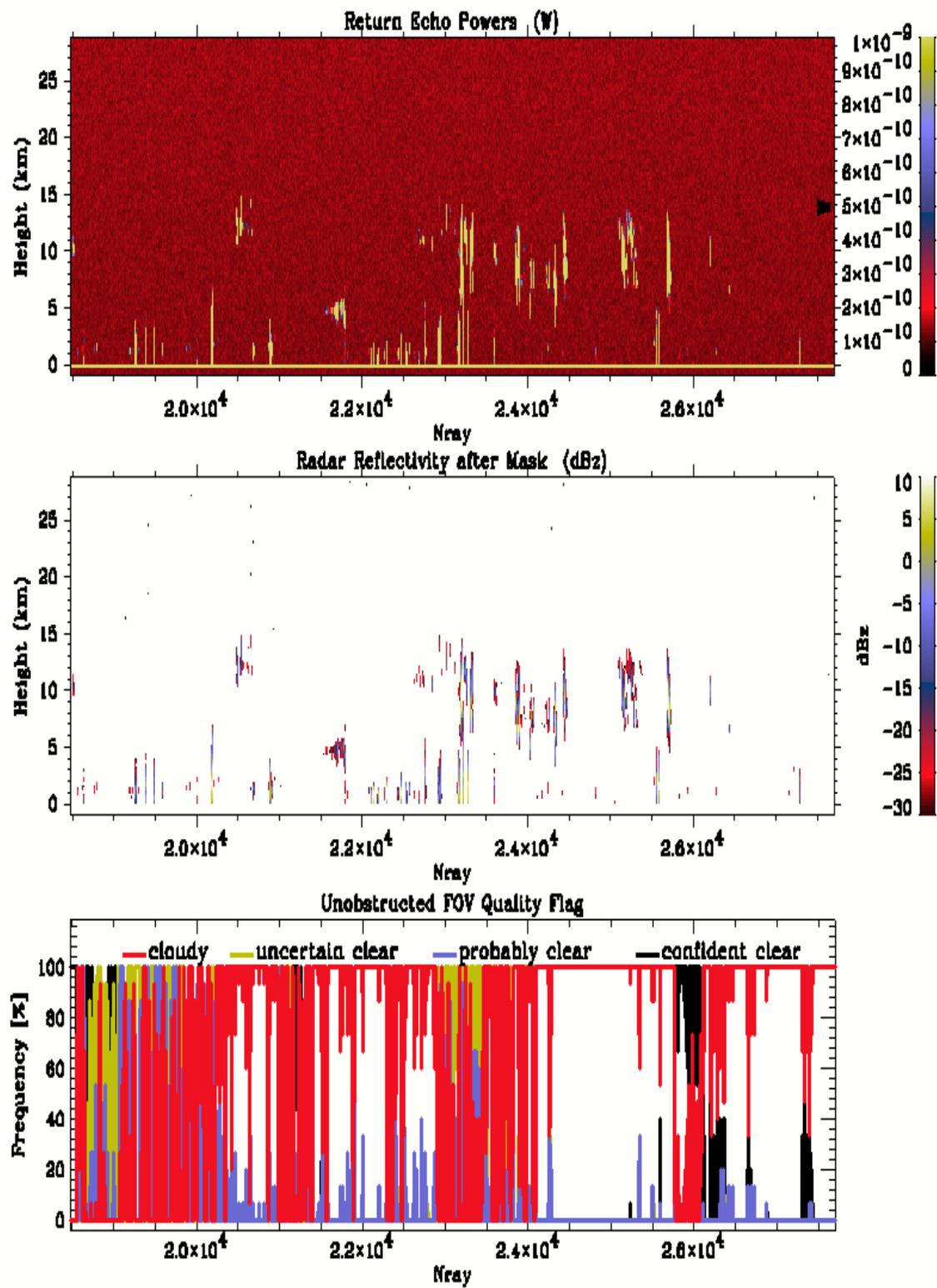
Figure 3(c). Return echo power before significant echo mask and radar reflectivity after mask (section 3).
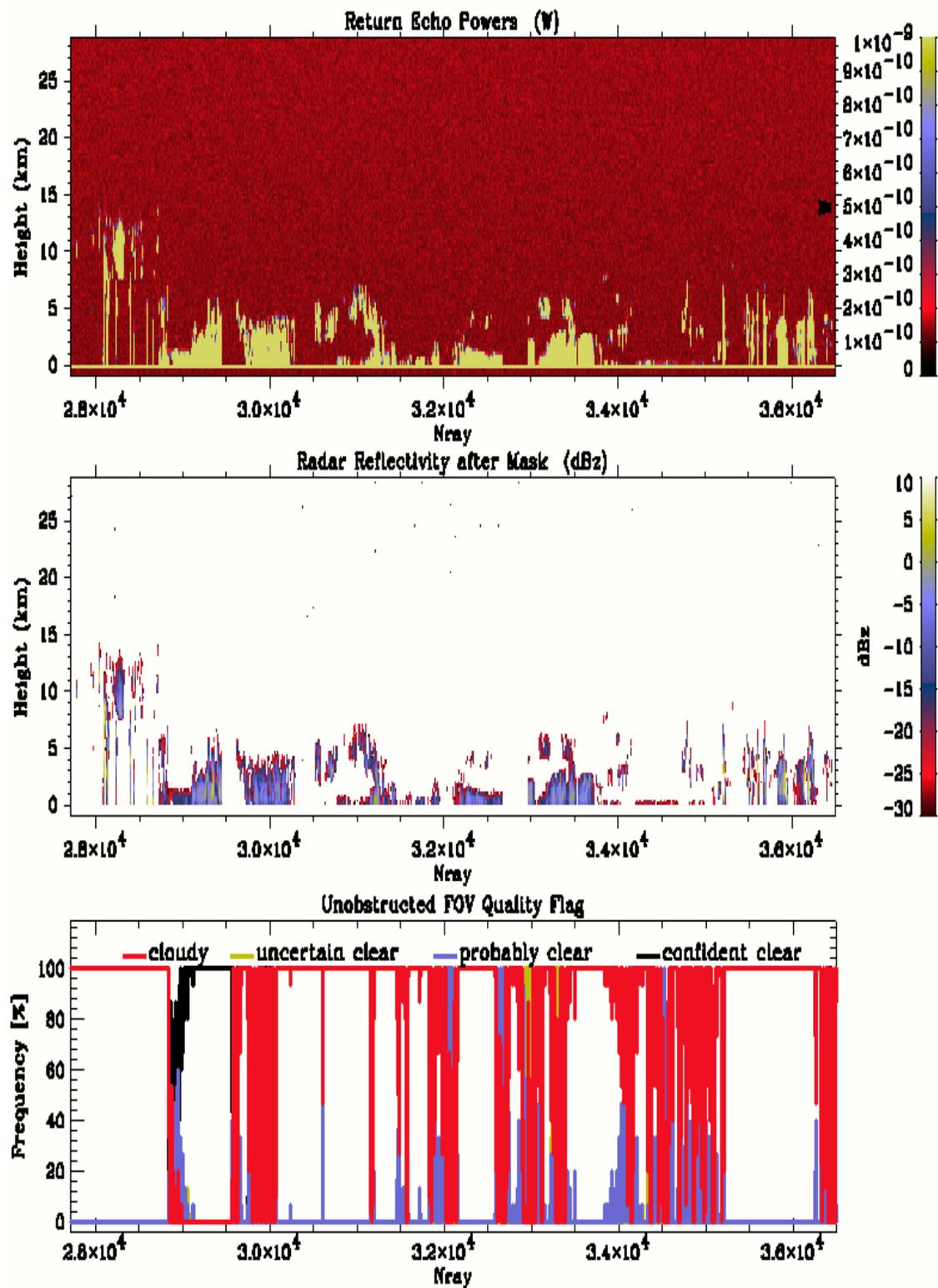
Figure 3(d). Return echo power before significant echo mask and radar reflectivity after mask (section 4).

B2. Diagnostic statistics ASCII output

Description of the ASCII file:

1. The first block of the ASCII output shows diagnostic statistics results of the CLOUDSAT profiles. It shows how many CloudSat rays (nray) and bins (nbin) were found in one orbit, which rays and bins are included in the diagnostic statistic analyses, and the number of cloudy profiles and how many profiles were found without cloud.

2. The second block shows the statistics of the MODIS 48 cloud mask bits.

   The first column is the number of the bytes for saving cloud mask information. The second column is the number of bits in each byte. There are 6 bytes for saving MODIS cloud mask information. Each byte has 8 bits. There are totally 48 bits are used for saving MODIS mask information. The third column shows the number of total bits.

   The fourth column shows the number pixels where bits are equal to zero. The fifth column shows the number of pixels where bits are equal to 1. Column 6 to 9 are used for bits 1-2 and bits 6-7.

3. Block 3 is for the frequency of occurrence of MODIS Cloud Classification. The first column is the type of MODIS Cloud Classification. The second column is the numerical designation Classification (see Table 3 for the definition). Column 3 to 10 are the frequency of MODIS Cloud Classification in eight different regions. The orbit is divided into following seven sections.

Orbit	– the whole orbit	
Tropic	– tropic	(23.5 S to 23.5 N)
N_Sub_Tropic	– north subtropics	(23.5 N - 35 N)
S_Sub_Tropic	– south subtropics	(23.5 S - 35 S)
N_Mid_Lat	– north middle latitude	(35 N - 55 N)
S_Mid_Lat	– south middle latitude	(35 S - 55 S)
N_High_Lat	– north high latitude	(55 N - 90 N)
S_High_Lat	– south high latitude	(55 S - 90 S)

4. Block 4 shows the statistics of CPR Echo Top Cloud Classification. The first column is the type of CPR Echo Top Cloud Classification. The second column is the numerical designation classification (see Table 4 for the definition). Column 3 to 10 are the number of CPR Echo Top Cloud Classifications in the eight different regions.

5. Block 5 shows the statistics of the MODIS CloudSat Scene Variability. The first and second columns are the type of MODIS CloudSat Scene Variability (see

Table 5 for the definition). Column 3 to 10 are the statistic number of MODIS CloudSat Scene Variability in eight different regions. Same as above, the orbit is divided into following seven sections for statistics.

The following is a sample of the diagnostic statistics ASCII output.

```
================================================================
===============    Statistic of CloudSat Profiles    =========
================================================================


nray (Profiles) =        36495
        nbin =          125

Profiles:    from              1 to         36495
Height:      from              1 to           125

Total profiles with cloud    :        18962
Total profiles without cloud :        17533


====================================================================================
=================                 MODIS cloud mask statistic      =================
 Byte  Bit  Tot          0           1           00         01        10         11
====================================================================================
    0    0    0       1206      546219
    0    1    1     343221      204204        311011      32210     56968     147236
    0    2    2     367979      179446
    0    3    3     266189      281236
    0    4    4     104268      443157
    0    5    5     113253      434172
    0    6    6     353019      194406        342978      10041     22276     172130
    0    7    7     365254      182171
    1    0    8      16193      531232
    1    1    9       1772      545653
    1    2   10       1510      545915
    1    3   11       7818      539607
    1    4   12       1369      546056
    1    5   13     117225      179484
    1    6   14     204170      343255
    1    7   15       3080      544345
    2    0   16      70227      211009
    2    1   17      26543      117116
    2    2   18     147425      286747
    2    3   19     202949      344476
    2    4   20     188585       77635
    2    5   21     138674      127487
    2    6   22       3162      271364
    2    7   23          0      272930
    3    0   24       1310      304114
    3    1   25     268255       28454
    3    2   26     541746        5679
    3    3   27     522368       25057
    3    4   28       1383      546042
    3    5   29       1376      546049
    3    6   30       1369      546056
    3    7   31       1369      546056
    4    0   32     503181       44244
    4    1   33     503294       44131
    4    2   34     503223       44202
    4    3   35     503194       44231
    4    4   36     503218       44207
    4    5   37     503087       44338
    4    6   38     503012       44413
    4    7   39     503147       44278
    5    0   40     503011       44414
    5    1   41     503152       44273
    5    2   42     503012       44413
    5    3   43     502863       44562
    5    4   44     502998       44427
```

```
   5    5    45      503063      44362
   5    6    46      502960      44465
   5    7    47      502971      44454
```

```
========================================================
=========  SUM of MODIS Cloud Classification  ========
========================================================
```

		Whole Orbit	Tropic	N_Sub_ Tropic	S_Sub_ Tropic	N_Mid _Lat	S_Mid _Lat	N_High _Lat	S_High _Lat
No Test	(0)	83	58	25	0	0	0	0	0
Clear	(1)	13596	3561	1757	299	2035	558	4144	1242
High Cloud	(2)	3757	244	298	0	325	0	1052	1838
High Cloud Very Thin	(3)	178	37	0	0	64	0	77	0
High Cloud Thin	(4)	73	60	2	0	0	0	0	11
High Cloud Think	(5)	3835	138	47	1	52	0	771	2826
Non High Cloud	(6)	8940	3464	201	893	886	2158	583	755
Mid Cloud Thick	(7)	1389	40	0	59	351	448	266	225
Low Cloud	(8)	0	0	0	0	0	0	0	0
Unclassifiable	(9)	4644	1975	24	1107	426	987	51	74

```
===============================================
=== SUM of CPR Echo Top Cloud Classification ===
===============================================
```

		Whole Orbit	Tropic	N_Sub_ Tropic	S_Sub_ Tropic	N-Mid _Lat	S_Mid _Lat	N_High _Lat	S_High _Lat
No Determination	(0)	0	0	0	0	0	0	0	0
Clear Profile	(1)	17533	4939	1202	839	2002	1932	2952	3667
High Cloud	(2)	9916	2676	1057	672	667	1380	1050	2414
Mid Level Cloud	(3)	3630	52	37	216	600	81	2092	552
Low Level Cloud	(4)	2174	1402	27	217	329	168	0	31
Multi Layer	(5)	3242	508	31	415	541	590	850	307

```
===============================================
=========  SUM of Scence Variability  ========
===============================================
```

		Whole Orbit	Tropic	N_Sub_ Tropic	S_Sub_ Tropic	N_Mid _Lat	S_Mid _Lat	N_High _Lat	S_High _Lat
No Determination		0	0	0	0	0	0	0	0
Highly Uniform	>= 0.9	21367	4210	1545	699	2895	1578	5177	5263
Uniform	>= 0.75	4049	1117	334	187	379	487	767	778
Low Uniform	>= 0.5	5989	2133	411	308	436	986	890	825
Variable	< 0.5	1473	621	40	92	224	338	96	62
Highly Variable	=< 0.25	3617	1496	24	1073	205	762	14	43

B3. Plots of the diagnostic statistics for quality assessment purposes

The following gives a sample of the diagnostic statistics plots for the quality assessment purposes.
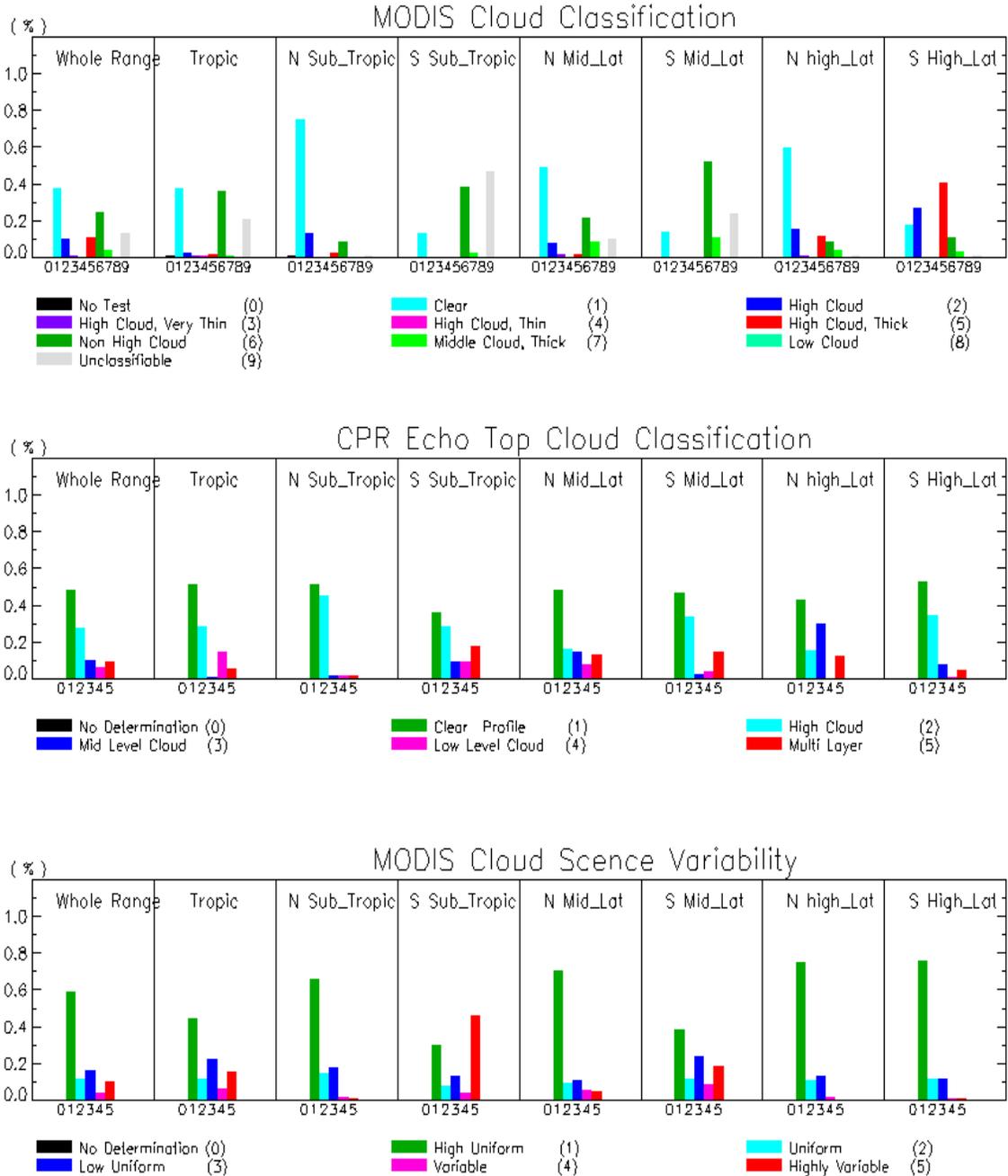

Figure 4. The diagnostic statistics plots. The upper panel is the MODIS cloud classification (block 3 in the diagnostic statistics ASCII output). The middle panel is CloudSat CPR echo top cloud classification (block 4 in the ASCII output). The lower panel is MODIS CloudSat scence variability (block 5 in the ASCII output).

Appendix C. Validation Data Set

		Date	Jun Day	Time (UTC)	Viewing Angle	MODIS File Name
TWPC2 Lat=-0.521 Lon=166.916						
1. Clear						
	1	12/2/2001	336	23:31:20	14.1	MOD35_L2.A2001336.2330.003.2001338163957.hdf
	2	11/25/2001	329	23:25:26	1	MOD35_L2.A2001329.2325.003.2001334083126.hdf
	3	9/20/2001	263	23:39:04	25.7	MOD35_L2.A2001263.2335.003.2001272030736.hdf
	4	8/21/2001	233	23:28:42	0.9	MOD35_L2.A2001233.2325.003.2001335011601.hdf
	5	8/3/2001	215	23:41:22	28.1	MOD35_L2.A2001215.2340.003.2001258155349.hdf
	6	9/6/2000	250	11:45:13	20.4	MOD35_L2.A2000250.1145.003.2001250065239.hdf
	7	11/5/2001	309	11:28:37	3.9	MOD35_L2.A2001309.1125.003.2001322203753.hdf
	8	9/25/2001	268	11:36:15	19.1	MOD35_L2.A2001268.1135.003.2001289232802.hdf
	9	9/20/2001	263	11:17:31	25.7	MOD35_L2.A2001263.1115.003.2001271023806.hdf
	10	9/11/2001	254	11:24:22	10.7	MOD35_L2.A2001254.1120.003.2001346013251.hdf
	11	8/10/2001	222	11:25:42	9.8	MOD35_L2.A2001222.1125.003.2001328030716.hdf
2. High Cloud						
	12	12/23/2001	357	11:27:11	4.3	MOD35_L2.A2001357.1125.003.2002039065540.hdf
3. High Cloud, Very Thin						
	13	11/16/2001	320	23:31:26	13	MOD35_L2.A2001245.1130.003.2001341194817.hdf
	14	11/12/2001	316	11:34:32	18.5	MOD35_L2.A2001316.1130.003.2001324214802.hdf
	15	10/29/2001	302	11:22:47	11.4	MOD35_L2.A2001302.1120.003.2001313115505.hdf
	16	9/9/2001	252	11:36:38	19.2	MOD35_L2.A2001252.1135.003.2001343230404.hdf
	17	9/2/2001	245	11:30:58	5.2	MOD35_L2.A2001245.1130.003.2001341194817.hdf
4. High Cloud, Thin						
	18	11/18/2001	322	23:19:02	17	MOD35_L2.A2001322.2315.003.2001327133012.hdf
	19	7/22/2001	203	23:17:08	28.7	MOD35_L2.A2001203.2315.003.2001317181416.hdf
	20	11/21/2001	325	11:27:48	3.2	MOD35_L2.A2001325.1125.003.2001328232553.hdf
	21	8/3/2001	215	11;19:47	23.7	MOD35_L2.A2001215.1115.003.2001322122607.hdf
5. High Cloud Thick						
	22	12/18/2001	352	23:30:13	12.7	MOD35_L2.A2001352.2330.003.2002038215217.hdf
	23	11/11/2001	315	23:13:24	29.6	MOD35_L2.A2001315.2310.003.2001324164130.hdf
	24	11/2/2001	306	23:19:46	16.5	MOD35_L2.A2001306.2315.003.2001320062545.hdf
	25	8/12/2001	224	23:35:02	14.9	MOD35_L2.A2001224.2335.003.2001327232849.hdf
	26	11/30/2001	334	11:22:01	10.6	MOD35_L2.A2001334.1120.003.2001338073225.hdf

27	11/14/2001	318	11:22:08	11.4	MOD35_L2.A2001318.1120.003.2001329013700.hdf
28	7/23/2001	204	11:38:14	19.6	MOD35_L2.A2001204.1135.003.2001315032740.hdf
29	7/18/2001	199	11:19:55	24.3	MOD35_L2.A2001199.1115.003.2001313115644.hdf

6. Non High Cloud

30	8/19/2001	231	23:40:57	28.2	MOD35_L2.A2001231.2340.003.2001308084902.hdf
31	8/19/2001	231	11:19:23	23.6	MOD35_L2.A2001231.1115.003.2001307211832.hdf

7. Mid Cloud Thick

32	12/25/2001	359	23:36:32	27.1	MOD35_L2.A2001359.2335.003.2002041072855.hdf
33	7/20/2001	201	23:29:15	1.7	MOD35_L2.A2001201.2325.003.2002198072112.hdf
34	12/16/2001	350	11:21:04	11.4	MOD35_L2.A2001350.1120.003.2002038042616.hdf
35	7/9/2001	190	11:26:07	11.1	MOD35_L2.A2001190.1125.003.2001309060431.hdf

8. Low Cloud

36	12/27/2001	361	23:24:24	2	MOD35_L2.A2001361.2320.003.2002042151155.hdf
37	12/13/2001	347	23:12:20	29.5	MOD35_L2.A2001347.2310.003.2002036023427.hdf
38	11/23/2001	327	23:37:41	27.4	MOD35_L2.A2001327.2335.003.2001333100239.hdf
X	11/7/2001	311	23:37:49	26.8	MOD35_L2.A2001311.2335.003.2001323191314.hdf
39	9/6/2001	249	23:27:53	1.1	MOD35_L2.A2001249.2325.003.2001343211226.hdf
40	7/18/2001	199	23:41:31	27.6	MOD35_L2.A2001199.2340.003.2001313215033.hdf
41	9/18/2001	261	11:29:54	3.4	MOD35_L2.A2001261.1125.003.2001273223347.hdf

9. Multi Layers

42	12/20/2001	354	23:17:42	17.6	MOD35_L2.A2001354.2315.003.2002041174722.hdf
43	9/13/2001	256	23:33:32	13.4	MOD35_L2.A2001256.2330.003.2001265010241.hdf
44	8/14/2001	226	23:22:46	14.9	MOD35_L2.A2001226.2320.003.2001330181610.hdf
45	8/5/2001	217	23:29:06	0.4	MOD35_L2.A2001217.2325.003.2001324023402.hdf
46	12/30/2001	364	11:33:14	18.9	MOD35_L2.A2001364.1130.003.2002044113522.hdf
47	12/25/2001	359	11:14:56	24.8	MOD35_L2.A2001359.1110.003.2002041014508.hdf
48	12/14/2001	348	11:33:27	18.5	MOD35_L2.A2001348.1130.003.2002036162613.hdf
49	11/28/2001	332	11:34:17	19.3	MOD35_L2.A2001332.1130.003.2001336063311.hdf
50	9/1/2000	245	11:26:54	23.3	MOD35_L2.A2000245.1125.002.2000318151119.hdf
51	9/1/2000	245	23:48:30	28.5	MOD35_L2.A2000245.2345.002.2000320052939.hdf
52	9/5/2000	249	23:24:07	27.9	MOD35_L2.A2000249.2320.002.2000265090156.hdf
53	9/8/2000	252	11:32:58	9.1	MOD35_L2.A2000252.1130.002.2000255110138.hdf
54	9/12/2000	256	23:30:01	14.6	MOD35_L2.A2000256.2330.002.2000266081517.hdf
55	9/19/2000	263	23:35:57	0.3	MOD35_L2.A2000263.2335.002.2000278094304.hdf
56	9/24/2000	268	11:32:33	9.7	MOD35_L2.A2000268.1130.002.2000271201205.hdf
57	9/26/2000	270	23:41:44	14.5	MOD35_L2.A2000270.2340.002.2000283123322.hdf

SGP

1. Clear

58	9/11/2000	255	17:39:48	2.9	MOD35_L2.A2000255.1735.002.2000272095244.hdf
59	1/8/2001	8	17:43:16	13.3	MOD35_L2.A2001008.1740.003.2001354195141.hdf
60	10/20/2000	294	17:44:48	13.6	MOD35_L2.A2000294.1740.002.2001057015152.hdf
61	1/24/2001	24	17:42:59	13.4	MOD35_L2.A2001024.1740.003.2001364035354.hdf
62	9/23/2001	266	17:24:46	10.4	MOD35_L2.A2001266.1720.003.2001287153007.hdf
63	11/22/2000	327	4:47:15	3.1	MOD35_L2.A2000327.0445.002.2000347081034.hdf
64	9/22/2001	265	4:40:16	2.9	MOD35_L2.A2001265.0440.003.2001275040422.hdf
65	9/13/2001	256	4:46:27	9.4	MOD35_L2.A2001256.0445.003.2001259092234.hdf
66	7/11/2001	192	4:48:19	9.5	MOD35_L2.A2001192.0445.003.2001251003940.hdf
67	4/8/2001	98	4:38:16	14.9	MOD35_L2.A2001098.0435.003.2001219235047.hdf

2. High Cloud

68	3/22/2001	81	17:35:28d	2.1	MOD35_L2.A2001081.1735.002.2001084080322.hdf
69	12/5/2000	340	17:55:33d	33	MOD35_L2.A2000340.1755.002.2000361124919.hdf
70	6/6/2001	157	17_58_23	42.2	MOD35_L2.A2001157.1755.003.2001161143820.hdf
71	11/27/2000	332	17_07_14	47.8	MOD35_L2.A2000332.1705.002.2000354110705.hdf
72	12/7/2000	342	17:43:23d	12.4	MOD35_L2.A2000342.1740.002.2000363030129.hdf
73	5/10/2001	130	4:37:38	14.5	MOD35_L2.A2001130.0435.003.2001242114039.hdf
74	3/30/2001	89	4:44:37	3.7	MOD35_L2.A2001089.0440.003.2001209082551.hdf

3. High Cloud Very Thin

75	12/23/2000	358	17:43:38d	13.5	MOD35_L2.A2000358.1740.002.2001011230416.hdf
76	11/30/2000	335	17:37:39d	1	MOD35_L2.A2000335.1735.002.2000357102644.hdf
77	5/27/2001	147	17:22:05d	21.4	MOD35_L2.A2001147.1720.003.2001154054824.hdf
78	4/9/2001	99	17_22_53	22.1	MOD35_L2.A2001099.1720.002.2001106093804.hdf
79	10/11/2000	285	17:51:00	24.5	MOD35_L2.A2000285.1750.002.2001056220103.hdf
80	9/19/2000	263	4:08:50	2.1	MOD35_L2.A2000263.0445.002.2000278002900.hdf
81	8/20/2000	233	4:36:51	24.4	MOD35_L2.A2000233.0435.002.2000235060143.hdf
82	2/17/2001	48	4:51:59	9.9	MOD35_L2.A2001048.0450.003.2001359104928.hdf
83	2/3/2001	34	4:40:00	14.2	MOD35_L2.A2001034.0435.003.2001362030649.hdf
84	1/7/2001	7	4:58:43	20.9	MOD35_L2.A2001007.0455.003.2001354022824.hdf
85	2/26/2001	57	4:45:40	3.1	MOD35_L2.A2001057.0445.003.2001310021808.hdf

4. High Cloud Thin

86	11/28/2000	333	17:49:55d	24.1	MOD35_L2.A2000333.1745.002.2000355075729.hdf
87	2/25/2001	56	17:42:25	13.7	MOD35_L2.A2001056.1740.003.2001309092009.hdf
88	2/11/2001	42	17:30:42	10.1	MOD35_L2.A2001042.1730.003.2001331041636.hdf
89	1/15/2001	15	17:48:59	23.8	MOD35_L2.A2001015.1745.003.2001357093748.hdf
90	5/16/2001	136	17:40;33	13.8	MOD35_L2.A2001136.1740.003.2001245212533.hdf

91	3/23/2001	82	4:38:39	14.8	MOD35_L2.A2001082.0435.003.2001190151708.hdf
92	6/9/2001	160	4:47:41	7	MOD35_L2.A2001160.0445.003.2001166015201.hdf

5. High Cloud Thick

93	3/6/2001	65	17:35:57d	1.3	MOD35_L2.A2001065.1735.002.2001070080140.hdf
94	4/3/2001	93	17:59:29d	41.6	MOD35_L2.A2001093.1755.002.2001095070337.hdf
95	4/20/2001	110	17:04:32d	47.4	MOD35_L2.A2001110.1700.002.2001116112434.hdf
96	2/18/2001	49	17:36:37	2	MOD35_L2.A2001049.1735.003.2001359175518.hdf
97	3/8/2001	67	17:23:33	22.2	MOD35_L2.A2001067.1720.003.2001179082107.hdf
98	11/15/2000	320	04_41_19	14.3	MOD35_L2.A2000320.0440.002.2000339200829.hdf
99	1/23/2001	23	4:58:20	20.7	MOD35_L2.A2001023.0455.003.2001362203751.hdf
100	1/16/2001	16	4:52:07	8.9	MOD35_L2.A2001016.0450.003.2001357165451.hdf
101	1/27/2001	27	4:33:57	25.2	MOD35_L2.A2001027.0430.003.2001365055955.hdf
102	2/8/2001	39	4:58:19	21.3	MOD35_L2.A2001039.0455.003.2001365025951.hdf

6. Non High Cloud

103	12/20/2000	355	17:13:04d	40.5	MOD35_L2.A2000355.1710.002.2001009113123.hdf

7. Mid Cloud Thick

104	11/7/2000	312	17:32:10	10.7	MOD35_L2.A2000312.1730.003.2001264020700.hdf
105	4/16/2001	106	17:28:57	10.7	MOD35_L2.A2001106.1725.003.2001226172531.hdf
106	11/8/2000	313	4:35:16	25.2	MOD35_L2.A2000313.0435.003.2001264064711.hdf
107	10/7/2000	281	4:35:55	25.1	MOD35_L2.A2000281.0435.003.2002003075154.hdf
108	9/15/2001	258	4:34:04	14.9	MOD35_L2.A2001258.0430.003.2001265090314.hdf

8. Low Cloud

109	2/9/2001	40	17:42:58	13.9	MOD35_L2.A2001040.1740.003.2001330025210.hdf
110	9/7/2001	250	17:25:24	10.1	MOD35_L2.A2001250.1725.003.2001345003707.hdf
111	3/29/2001	88	17:41:30	13.3	MOD35_L2.A2001088.1740.003.2001208080820.hdf
112	5/18/2001	138	17:28:18	10.4	MOD35_L2.A2001138.1725.003.2001246065719.hdf
113	10/21/2000	295	4:47:54	2.3	MOD35_L2.A2000295.0445.003.2002007095638.hdf
114	9/24/2001	267	4:28:01	25.2	MOD35_L2.A2001267.0425.003.2001285155535.hdf

9. Multi Layers

115	9/5/2001	248	17:37:40	14	MOD35_L2.A2001248.1735.003.2001343115347.hdf
116	2/27/2001	58	17:30:09	10.4	MOD35_L2.A2001058.1730.003.2001309165146.hdf
117	8/22/2001	234	17:26:13	9.6	MOD35_L2.A2001234.1725.003.2001336034906.hdf
118	9/16/2001	259	17:18:40	22.2	MOD35_L2.A2001259.1715.003.2001279091540.hdf
119	2/24/2001	55	4:57:55	21.1	MOD35_L2.A2001055.0455.003.2001309164709.hdf
120	9/6/2001	249	4:40:47	3	MOD35_L2.A2001249.0440.003.2001343011449.hdf

NSA

1. Clear

121	3/6/2000	66	22:57:14	5.3	MOD35_L2.A2000066.2255.003.2002185042808.hdf
122	12/24/2000	359	23:13:24	18.3	MOD35_L2.A2000359.2310.003.2001285102716.hdf
123	12/23/2000	358	22:30:37	11.3	MOD35_L2.A2000358.2230.003.2001284213848.hdf
124	3/12/2000	72	22:20:25	20.7	MOD35_L2.A2000072.2220.003.2002125071724.hdf
125	10/9/2000	283	22:50:15	2	MOD35_L2.A2000283.2250.003.2002005145140.hdf
126	12/28/2000	363	7:49:27	16.6	MOD35_L2.A2000363.0745.003.2001288085409.hdf
127	1/1/2001	1	7:24:54	1	MOD35_L2.A2001001.0720.003.2001296172744.hdf
128	10/9/2000	283	7:50:48	16.6	MOD35_L2.A2000283.0750.003.2002005104548.hdf
129	10/13/2000	287	7:26:18	1.4	MOD35_L2.A2000287.0725.003.2002005194710.hdf
130	10/15/2000	289	7:14:02	9.5	MOD35_L2.A2000289.0710.003.2002007052300.hdf

2. High Cloud

131	3/4/2000	64	23:09:25	13.6	MOD35_L2.A2000064.2305.003.2002122121732.hdf
132	1/7/2001	7	23:25:16	25.3	MOD35_L2.A2001007.2325.003.2001354103957.hdf
133	1/15/2001	15	22:35:58	7.2	MOD35_L2.A2001015.2235.003.2001357113121.hdf
134	2/9/2001	40	22:29:57	11.3	MOD35_L2.A2001040.2225.003.2001330040046.hdf
135	2/15/2001	46	6:53:37	21.2	MOD35_L2.A2001046.0650.003.2001359202537.hdf
136	1/10/2001	10	7:18:31	5.9	MOD35_L2.A2001010.0715.003.2001355131310.hdf
137	1/15/2001	15	7:36:33	7.6	MOD35_L2.A2001015.0735.003.2001357063351.hdf

3. High Cloud Very Thin

138	2/5/2001	36	22:54:28	6.6	MOD35_L2.A2001036.2250.003.2001364085521.hdf
139	3/15/2001	74	23:53:57	39.3	MOD35_L2.A2001074.2350.003.2001185002714.hdf
140	12/21/2000	356	7:43:26	12.2	MOD35_L2.A2000356.0740.003.2001294095937.hdf
141	12/27/2000	362	7:06:39	13.6	MOD35_L2.A2000362.0705.003.2001287174041.hdf
142	2/9/2001	40	7:30:23	4.1	MOD35_L2.A2001040.0730.003.2001329235442.hdf
143	2/11/2001	42	7:18:07	5.6	MOD35_L2.A2001042.0715.003.2001332184929.hdf
144	2/17/2001	48	6:41:21	27.9	MOD35_L2.A2001048.0640.003.2001358114539.hdf

4. High Cloud Thin

145	11/25/2000	330	7:07:03	13.7	MOD35_L2.A2000330.0705.003.2001276231706.hdf
146	3/4/2000	64	8:09:58	28.8	MOD35_L2.A2000064.0805.003.2002122034921.hdf
147	3/5/2000	65	7:14:53	9.2	MOD35_L2.A2000065.0710.003.2002122122314.hdf
148	3/16/2001	75	7:59:37	24.3	MOD35_L2.A2001075.0755.003.2001185060017.hdf

5. High Cloud Thick

149	1/18/2001	18	23:06:21	14.2	MOD35_L2.A2001018.2305.003.2001359092723.hdf
150	3/17/2001	76	22:04:10	27.8	MOD35_L2.A2001037.0655.003.2001364160352.hdf
151	3/25/2000	85	6:51:13	24.1	MOD35_L2.A2000085.0650.003.2002049180857.hdf

152	2/6/2001	37	6:59:56	17.5	MOD35_L2.A2001037.0655.003.2001364160352.hdf
153	3/16/2001	75	6:21:51	36.8	MOD35_L2.A2001075.0620.003.2001185051826.hdf
154	3/18/2001	77	7:47:30	16.1	MOD35_L2.A2001077.0745.003.2001186165421.hdf
155	3/20/2001	79	7:35:16	7.5	MOD35_L2.A2001079.0735.003.2001187214658.hdf

6. Non High Cloud

156	11/30/2000	335	22:24:38	16	MOD35_L2.A2000335.2220.003.2001279082910.hdf
157	12/28/2000	363	22:48:53	2.4	MOD35_L2.A2000363.2245.003.2001288214405.hdf
158	3/20/2001	79	22:34:43	7	MOD35_L2.A2001079.2230.003.2001188102030.hdf
159	1/19/2001	19	7:11:59	9.8	MOD35_L2.A2001019.0710.003.2001359161934.hdf
160	1/28/2001	28	7:06:00	13.7	MOD35_L2.A2001028.0705.003.2001365222207.hdf
161	1/31/2001	31	7:36:35	7.9	MOD35_L2.A2001031.0735.003.2002002101445.hdf

7. Mid Cloud Thick

162	1/10/2001	10	22:17:48	20.1	MOD35_L2.A2001010.2215.003.2001356013024.hdf
163	12/23/2000	358	7:31:10	3.4	MOD35_L2.A2000358.0730.003.2001284145005.hdf
164	9/18/2000	262	7:33:16	4	MOD35_L2.A2000262.0730.003.2001337144123.hdf
165	12/4/2000	339	7:00:27	17.8	MOD35_L2.A2000339.0700.003.2001280131336.hdf
166	9/2/2000	246	7:33:33	4	MOD35_L2.A2000246.0730.003.2001350084631.hdf
167	3/26/2000	86	7:34:05	4.5	MOD35_L2.A2000086.0730.003.2002050223227.hdf
168	4/6/2000	97	7:15:33	8.8	MOD35_L2.A2000097.0715.003.2002048173042.hdf
169	9/4/2000	248	7:21:17	4.7	MOD35_L2.A2000248.0720.003.2001350171431.hdf

8. Low Cloud

170	9/23/2000	267	22:50:52	2.1	MOD35_L2.A2000267.2250.003.2002124123157.hdf
171	1/1/2001	1	22:24:19	15.6	MOD35_L2.A2001001.2220.003.2001297000816.hdf
172	4/27/2000	118	22:34:14	11.6	MOD35_L2.A2000118.2230.003.2002068221554.hdf
173	10/18/2000	292	22:44:02	2.5	MOD35_L2.A2000292.2240.003.2002008214029.hdf
174	4/16/2000	107	22:52:05	1.9	MOD35_L2.A2000107.2250.003.2002056173600.hdf
175	11/5/2000	310	7:31:50	3.4	MOD35_L2.A2000310.0730.003.2001263002613.hdf
176	8/1/2000	214	7:32:44	3.6	MOD35_L2.A2000214.0730.003.2002118195432.hdf
177	10/20/2000	294	7:32:21	3.8	MOD35_L2.A2000294.0730.003.2002106150417.hdf
178	9/20/2000	264	7:21:01	5.3	MOD35_L2.A2000264.0720.003.2002126045357.hdf
179	11/7/2000	312	7:19:35	5.5	MOD35_L2.A2000312.0715.003.2001263224550.hdf
180	12/16/2000	351	7:24:59	1.3	MOD35_L2.A2000351.0720.003.2001292153532.hdf
181	10/29/2000	303	7:25:53	2.1	MOD35_L2.A2000303.0725.003.2002025231041.hdf
182	11/30/2000	335	7:25:13	2.2	MOD35_L2.A2000335.0725.003.2001279015904.hdf

9. Multi Layers

183	3/26/2000	86	22:33:33	11.8	MOD35_L2.A2000086.2230.003.2002052094713.hdf
184	4/7/2000	98	22:58:10	5.8	MOD35_L2.A2000098.2255.003.2002049171835.hdf
185	5/6/2000	127	22:27:40	15.7	MOD35_L2.A2000127.2225.003.2002066163351.hdf
186	7/10/2000	192	23:09:53	14.5	MOD35_L2.A2000192.2305.003.2002113004701.hdf

187	12/19/2000	354	22:55:09	6.3	MOD35_L2.A2000354.2255.003.2001293214925.hdf
188	4/20/2000	111	7:28:20	0.3	MOD35_L2.A2000111.0725.003.2002063135513.hdf
189	3/28/2000	88	7:21:52	4.6	MOD35_L2.A2000088.0720.003.2002053121229.hdf
190	3/19/2000	79	7:27:31	1.8	MOD35_L2.A2000079.0725.003.2002130094700.hdf
191	5/24/2000	145	7:15:26	9.6	MOD35_L2.A2000145.0715.003.2002082123734.hdf
192	12/17/2000	352	8:07:56	28.5	MOD35_L2.A2000352.0805.003.2001293011558.hdf
193	1/13/2001	13	7:48:52	16.4	MOD35_L2.A2001013.0745.003.2001356031952.hdf